Session D. Measurements of Microwave Radiation

Chairman: *A. W. Guy*
Vice-Chairman: *P. Czerski*
Rapporteurs: *R. C. Baird* and *M. Piotrowski*

QUANTITATION OF INDUCED ELECTROMAGNETIC FIELD PATTERNS IN TISSUE AND ASSOCIATED BIOLOGIC EFFECTS

A. W. Guy

Department of Rehabilitation Medicine, University of Washington, School of Medicine, Seattle, Washington, U. S. A.

INTRODUCTION

It is the desire of both the users and those who regulate the use of electromagnetic (EM) power to promulgate exposure guides that are conservative enough to insure the safety of man but do not unnecessarily restrict the application of the energy for the benefit of man. Such guides must be based on a quantitative understanding of the relationship between any biologic effect or damage, the fields induced in the affected tissue, and the fields in the environment of the exposed subject. In order to properly evaluate the hazard, it is also necessary to determine whether an observed effect is due to indirect thermal action, or whether it is directly related to the fields induced in the subject. Thus, a quantitative description of the EM fields within the tissues and an understanding of the relationship between these fields and the thermodynamics of the biologic system are desirable. The latter also provides a basis for useful instrumentation techniques for determining absorbed power densities and induced fields in the tissues of the exposed subjects by simple temperature measurements.

THERMAL CONSIDERATIONS

The energy equation for the time rate of change of temperature (°C sec) per unit volume of subcutaneous tissue in a subject exposed to EM fields is $dT/dt = 0.239 \times 10^{-3}/c\ [W_a + W_m - W_c - W_b]$ where W_a is the absorbed power density, W_m is the metabolic heating rate, W_c is the heat loss due to thermal conduction, W_b is

WHO – Biologic effects & health hazards of microwave radiation
1974

the power dissipated by blood flow, all expressed in W/kg, and c is the thermal conductivity expressed in kcal/kg $-^{\circ}$C. The absorbed power density for tissue exposed to an EM field is $W_a = 10^{-3}\sigma/\varrho E^2$ where σ is the electrical conductivity in mhos/meter, ϱ is the tissue density in g/cm^3, and E is the rms value of the electric field (V/m) in the tissue. If it is assumed that blood enters the tissue at arterial temperature T_a and leaves at tissue temperature T, we may express blood cooling by $W_b = k_2 m\, c_b/\varrho_b \Delta T'$ where $\Delta T' = T - T_a$, c_b is the specific heat of blood, ϱ_b is the density of blood, m is the blood flow rate in ml/100 g-min, and the constant $k_2 = 0.698$. Prior to the time the tissue is exposed to fields, it is assumed that a steady state condition exists where $W_a = dT/dt = 0$ requiring $W_m = W_c + W_b$. According to the typical values of the physical and thermal properties of tissues given in Table 1, under normal conditions the metabolic rate W_m averages 1.3 W/kg for the total body, 11 W/kg for brain tissue, and 33 W/kg for heart tissue. According to the energy equation, we would expect to see some change in tissue temperature due to applied EM fields if the power absorption density W_a were of the same order of magnitude as W_m or more. In fact, the safety guides in the United States that allow a maximum human exposure level of 10 mW/cm^2 of incident power are partially based on limiting the average W_a to the average resting value of W_m. Thus, absorbed power densities $W_a >> W_m$ could be expected to produce marked thermal effects, whereas power densities $W_a << W_m$ would not be expected to produce any significant thermal effects. Safety guides, how-

Table 1

Thermal and physical properties of human tissues

Tissue	Subscript	Specific heat (c) kcal/kg	Density σ(1) g/cm^3	Metabolic rate (W_o) W/kg	Blood flow rate (m) ml/100 g · min	Thermal conductivity (k_c) kcal/kg– °C
skeletal muscle (excised)	m	0.83	1.07			4.4
skeletal muscle (living)	m			0.7	2.7	6.42
fat	f	0.54	0.937			2.1(1)
bone (cortical)	bc	0.3	1.79			14.6(1)
bone (spongy)	bs	0.71	1.25			
blood	bl	0.93	1.06(2)			5.06
heart muscle	m			33	84	
brain (excised)						5.0
brain (living)	br			11	54	8.05
kidney	k			20	420	
liver	l			6.7	57.7	
skin (excised)	s					2.5
skin (living)				1	12.8	4.42
whole body				1.3	8.6	

(1) For pig
(2) For humans

WHO – BIOLOGIC EFFECTS & HEALTH HAZARDS OF MICROWAVE RADIATION 1974

ever, are not, and cannot be, specified in terms of absorbed power density, but are more conveniently expressed for radiation fields in terms of an incident power flux density expressed in units of mW/cm² or, for the case of stationary or quasi-stationary fields, they may be expressed in terms of electric field strength E, in V/m, or magnetic field strength H, in a/m. The latter two quantities can also be expressed in terms of stored energy density, $\varepsilon_o E^2$ or $\mu_o H^2$, where ε_o is the permittivity and μ_o is the permeability of free space. It is virtually impossible, however, to classify any of the above field quantities measured exterior to an exposed subject as being hazardous, non-hazardous, thermal, or non-thermal, without first knowing enough about exposure conditions, frequency, subject size, and subject geometry to determine what the absorbed power density in the subject actually is. Peak values of absorbed power density 50 W/kg $\leq W_a \leq$ 170 W/kg have been used to provide vigorous therapeutic heating of deep vasculated tissues in man treated with diathermy (4), and values of $W_a \geq 4$ W/kg absorbed in brain tissue of cats provided measureable increases in brain temperature and decreases in latency times of evoked potentials (6). Body temperature increases, accompanied by behavioral changes, have been observed in rats by Justesen (7), for $W_a \geq 3.1$ W/kg, and by Hunt et al. (5), for $W_a \geq 6.3$ W/kg, averaged over the body of the animal. Changes in body temperature, thermoregulatory, cardiovascular, and metabolic characteristics were observed by Philips et al., (10) for rats exposed to fields such that $W_a = 6.3$ W/kg averaged over the body of the animal. Cataracts have been induced in rabbits by acute exposures where power absorption density in the eye was greater than 138 W/kg accompanied by marked increases in temperature (8).

FORCE EFFECTS

In addition to tissue heating, electromagnetic energy can produce forces at the surface of an exposed subject, forces across internal tissue, or cell interfaces, and pressure changes in body fluids proportional to E². Schwan (12) has shown that one such effect, pearl chain formation of suspended particles in a fluid, can only occur in a biologic medium at field levels that are also thermally damaging. Both thermal effects and pearl chain formation, which depends on a sustained force, are related to average power absorption and do not relate to the peak absorbed power from modulated or pulsed EM fields. On the other hand, the evoked auditory effects in man and animals appear to be related to the instantaneous value of pulsed fields at average field levels that are far below those capable of producing temperature changes in the tissues. Frey (1) has found the loudness of the effect in humans to be proportional to peak power for pulse widths greater than 60, whereas Guy et al. (2) have found the threshold for the evoked responses in humans and cats to be related to the energy per pulse (20 to 40 μJ/cm² incident energy density or of the order of 15 mJ/kg absorbed energy) for pulse widths from 1 to 30 μs, regardless of average and peak power. Whether these effects are due to impulsive field forces or some other unexplained interaction has not been determined.

RELATIONS BETWEEN INCIDENT FIELDS AND POWER ABSORPTION DENSITY

Considerable insight can be gained into the relationship between frequency, body size, and absorbed power by considering spherical tissue layers exposed to a plane electromagnetic wave. Figure 1 illustrates the relative absorbed power density patterns

WHO – Biologic effects & health hazards of microwave radiation 1974

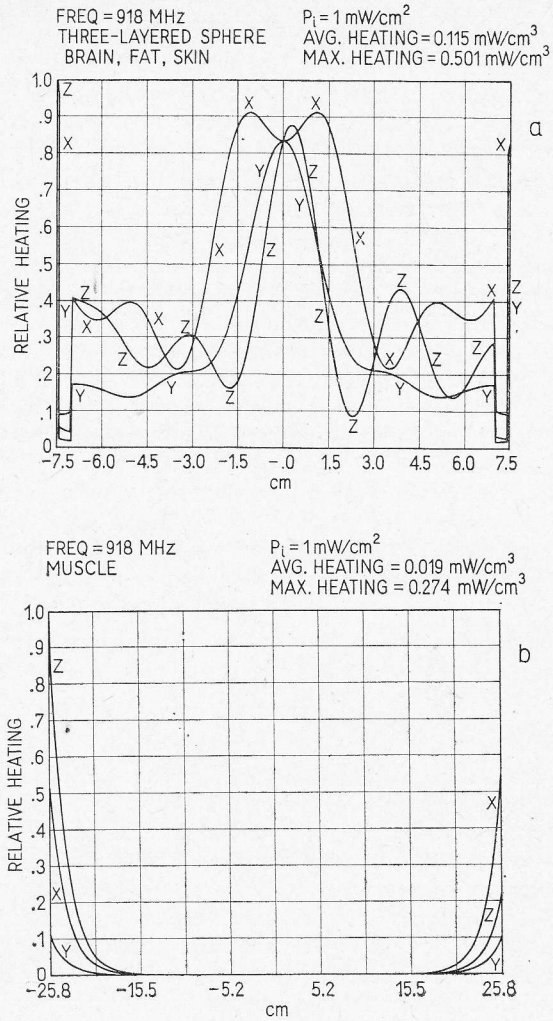

Fig. 1. Power absorption densities in spherical tissue layers exposed to 1 mW/cm² incident plane wave power density. a. Spherical model of human head with brain core surrounded by thin layers of bone and skin exposed to 918 MHz radiation (radius in the order af a wavelength in tissue). b. Spherical homogenous muscle model simulating man exposed to 918 MHz radiation (radius large compared with a wavelength with tissue).

for various spherical tissue geometries exposed to a 1 mW/cm² plane wave source. The origin of the rectangular coordinate system used in the figures is located at the center of the sphere with wave propagation along the z axis and the E field polarized along the x axis. The maximum absorption and the average absorption density are tabulated on each plot. When the diameter of the exposed object is of the order of one wavelength as measured in the tissue, severe internal wave interference produces sharp maxima and minima in the power absorption patterns as shown in Figure 1a for a sphere representing a human head exposed to 918 MHz radiation. The spherical model is composed of an inner core consisting of brain tissue surrounded by a layer of bone and skin.

WHO – Biologic effects & health hazards of microwave radiation 1974

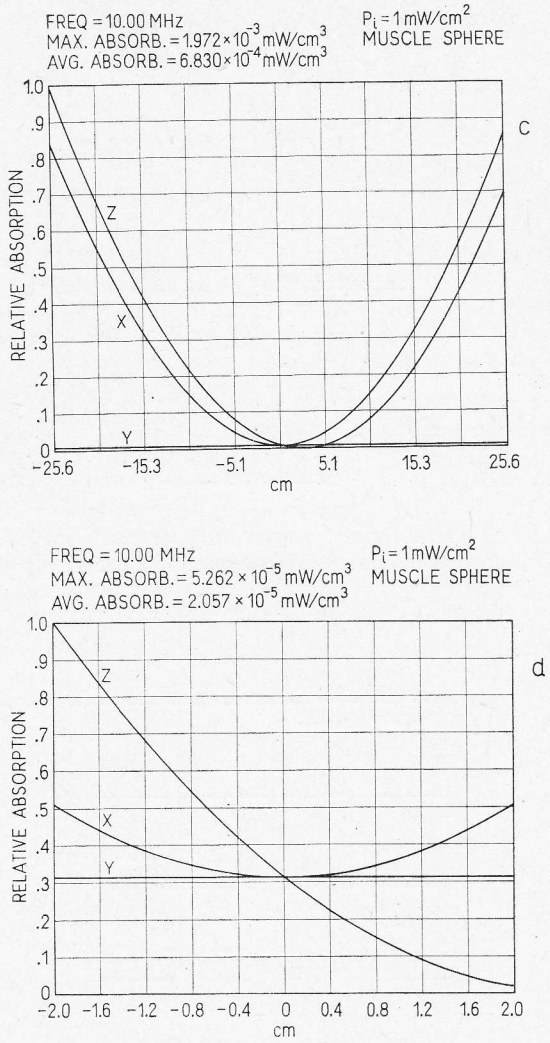

Fig. 1. c. Spherical homogeneous muscle model simulating man exposed to 10 MHz radiation (radius small compared with a wavelength in tissue). d. Spherical homogenous muscle model simulating a mouse exposed to 10 MHz radiation (radius small compared with a wavelength in tissue).

When the object is large compared with a wavelength, as measured in the tissue, the maximum absorption occurs at the exposed surface, decaying nearly exponentially with depth as shown in Figure 1b for a homogeneous muscle sphere with the same mass as a 70 kg man exposed to 918 MHz radiation. When the exposed subject is very small compared with a wavelength, but of a mass approximating that of man, the power absorption density varies nearly as the square of distance from the y axis (direction of magnetic field vector) as shown in Figure 1c. On the other hand, if the object is very small compared with a wavelength, but with a small mass, the power absorption density is uniform along the y axis but increases with distance toward the exposed surface and

WHO – Biologic effects & health hazards of microwave radiation 1974

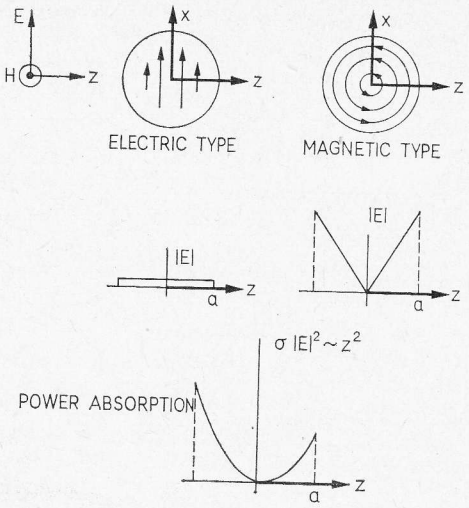

Fig. 2. Sketch depicting how electric and magnetically induced electric fields add in exposed tissue sphere to produce absorbed power distribution pattern.

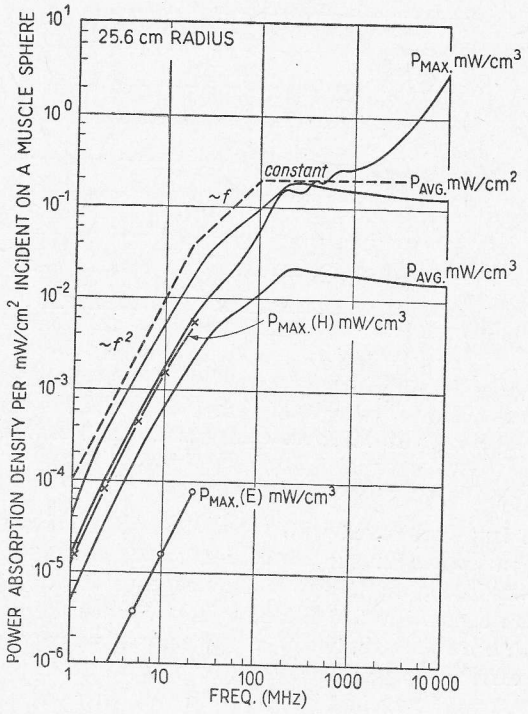

Fig. 3. Power absorption density patterns versus frequency in spherical muscle model of 70 kg man exposed to plane wave 1 mW/cm² source.

WHO – Biologic effects & health hazards of microwave radiation
1974

decreases with distance toward the opposite surface, as shown in Figure 1 d. The latter two absorption patterns for objects small compared with a wavelength can be explained from simple quasistatic field theory (9). The electric field component of the incident plane wave couples to the object in the same manner as a static electric field giving rise to a constant internal electric field which is $3/\varepsilon$ times smaller, and in the same direction as the applied field, where $\varepsilon >> 1$ is the dielectric constant of the tissue. Superimposed on the constant internal electric field is another magnetically induced electric field component encircling the y axis as shown in Figure 2. The magnitude of the latter field, which varies directly with radial distance r from the axis, and directly with frequency f, is given by $E = \pi frH$, where H is the magnetic field. The H-induced E field component in a man-size sphere is much greater than the E-induced component, whereas, for a small mouse-size object both components are significant. The variation of the maximum and average power absorption density with frequency for an exposed homogeneous muscle sphere with the same volume is shown in Figure 3. Also shown in the figure is the average power absorption density per unit total surface area of the sphere. In the frequency range from 1 MHz to 20 MHz, the absorption characterized by the pattern in Figure 2 c varies as the square of the frequency. This is due primarily to the magnetically induced fields. The maximum power absorption density induced by the incident H field is denoted by the curve marked with crosses, and that due to the incident E field is denoted by the curve with zeros in the range where the quasistatic coupling approximations apply. Note that in this range, the maximum power absorption density is only 10^{-5} to 10^{-2} W/kg per mW/cm² of incident power. In the frequency range 100 to 1000 MHz, internal reflections are significant for the man-size sphere and the average absorption attains a maximum of 2×10^{-2} W/kg per mW/cm² of incident power at 200 MHz, which remains relatively constant with frequency up to 10 GHz. The maximum absorption density increases with frequency above 1000 MHz, approaching that produced by non-penetrating radiation. The dashed lines illustrate roughly the frequency dependence of the total or average absorbed power and how safety standards might be relaxed as a function of frequency if the absorption charac-

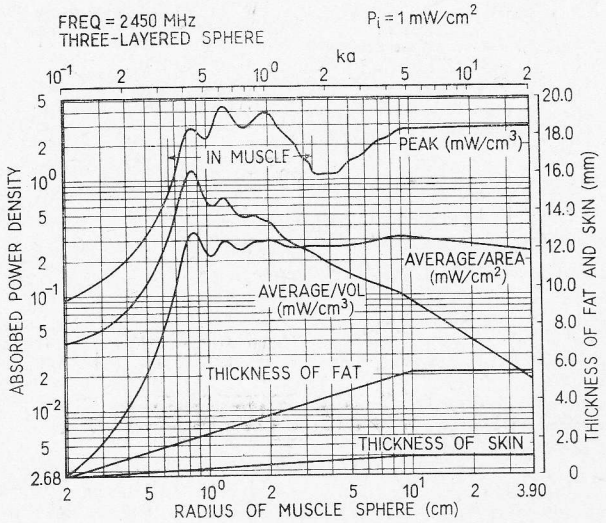

Fig. 4. Power absorption density versus outside radius in spherical tissue layer model of animal exposed to 2450 MHz 1 mW/cm² plane wave.

WHO – BIOLOGIC EFFECTS & HEALTH HAZARDS OF MICROWAVE RADIATION 1974

teristics in man were the same as for the sphere. The wide variation of absorption characteristics with body size is illustrated in Figure 4 for a sphere consisting of an inner muscle core surrounded by concentric layers of subcutaneous fat and skin exposed to 2450 MHz plane wave 1 mW/cm² radiation. The total radius, fat thickness and skin thickness are noted on the figure. It is significant to note that based on the spherical models, the peak power absorption could be as high as 4.2 W/kg in the body or head of a small bird or animal but as low as 0.27 W/kg at the surface, and 0.05 W/kg 2.5 cm deep in the human body exposed to a 1 mW/cm², 918 MHz source (Figure 1b). Thus, 10 mW/cm² could be of extreme and 0.5 mW/cm² could be of mild thermal significance to the smaller animal in comparison with metabolic rate. For the human model, on the other hand, 10 mW/cm² would appear to be of mild thermal significance and 0.5 mW/cm² would have negligible thermal significance.

MEASUREMENT OF ABSORBED POWER DENSITY

Though the sphere analysis provides some insight into the size and frequency dependence of absorption characteristics of the subject, it is not a substitute for quantifying the actual absorption in irregular body shapes. Electromagnetic fields or quantities related to the fields can be measured both *in situ* and *in vivo* in test animals or even humans by means of implanted microwave diodes, thermocouples, and thermistors. Thermocouples and thermistors were used extensively in the past for measuring the temperature rise in tissues exposed to radiation. There are several problems associated with the use of thermocouples or thermistors to ascertain absorbed power: 1) the element senses only the temperature of the tissue which is also a function of other mechanisms such as thermal diffusion, blood flow, and the thermoregulatory characteristics of the animal; 2) if the sensor is left in the tissue during irradiation, it can be directly heated by the RF fields or it can significantly modify the fields and the associated temperature rises; and 3) the sensor is relatively insensitive to low power densities.

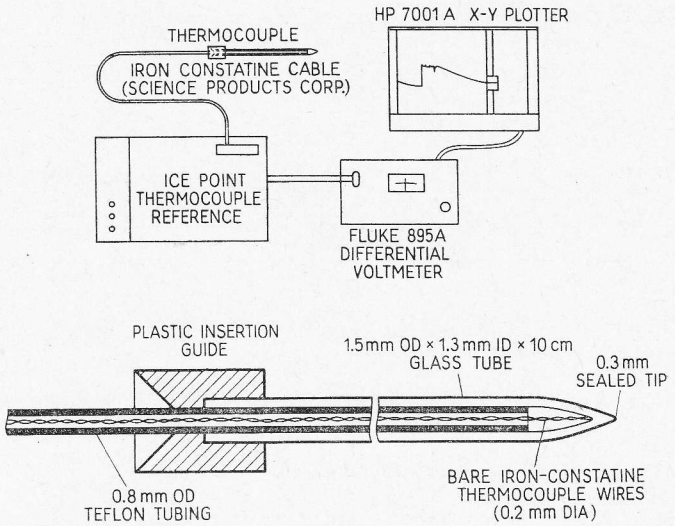

Fig. 5. Apparatus used for determining power absorption density in biological tissue by a thermocouple.

WHO – Biologic effects & health hazards of microwave radiation
1974

All of these problems can be eliminated through a technique that utilizes a small diameter plastic or glass tube sealed at one end and implanted at the location where a measurement of the absorbed power is desired. The tube, illustrated in Figure 5, is long enough so that the open end, fitted with a plastic guide, protrudes from the tissue. A very small diameter thermocouple is inserted into the tube with the sensor located at the probe tip and an initial temperature is recorded. The thermocouple is quickly withdrawn from the tube and the animal is exposed under the normal conditions of the experimental protocol with the following exceptions. Instead of using the power level normally chosen for a given experiment, a very high power burst of radiation of duration sufficient to produce a rapid but safe temperature rise in the tissue is applied to the animal. The thermocouple is then rapidly returned to its original position and the new temperature is recorded for several minutes. The temperature versus time curve is then extrapolated back in time to the period when the power was applied and, based on the density and specific heat of the tissue, the absorbed power density is calculated from the difference between initial and final extrapolated temperatures. The short exposure period insures that there is no loss of heat due to cooling or diffusion, so integration of the energy equation over the short time period t gives $W_a = 4.186 \times 10^3 c\Delta T/t$ where c is the specific heat of the tissue, ΔT the temperature change in degrees Celsius, and t the time of exposure in seconds. The measured absorbed power can then be used to relate the input power of the source to the absorbed power in the tissue under normal lower power exposure conditions. Figure 6 illustrates the measured absorbed power density in the eyes of rabbits exposed to the near zone field of a 2450 MHz diathermy applicator measured by this technique. The results have been used to establish the relationship between internal absorbed power and cataractogenesis (6). Guy (3), (6), has described a method for rapid evaluation of absorbed power density in tissues of arbitrary shape and characteristics when they are exposed to various sources, including plane wave, aperture, slot, and dipoles. The method, valid for both far- and near-zone fields, involves the use of a thermograph camera for recording temperature distributions produced by energy absorption in phantom models of the tissue structures. The absorbed power or magnitude of the electric field may then be obtained anywhere on the model as a function of the square root of the magnitude of the calculated heating pattern. The phantoms are composed of materials with dielectric

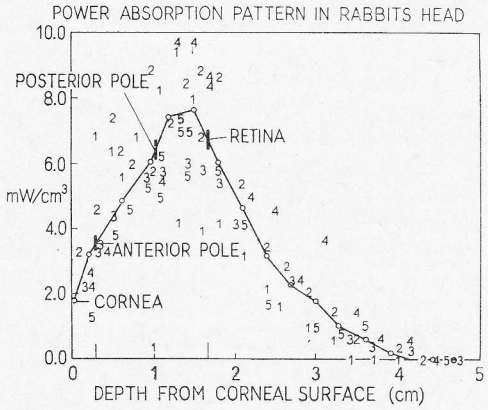

Fig. 6. Power absorption density in the eye and head of a rabbit exposed to 2450 MHz diathermy "O" director measured by a thermocouple method (values normalized to 1 watt input to applicator or 8.42 mW/cm² incident). Solid line is the mean of 5 rabbits.

WHO – Biologic effects & health hazards of microwave radiation 1974

and geometric properties identical to the tissue structures they represent. Phantom materials have been developed which simulate human fat, muscle, brain, and bones. These materials have complex dielectric properties that closely resemble the properties of human tissues reported by Schwan (11). The modeling material for fat may also be used for bone. The synthetic muscle can also be used to simulate other tissues with high water content. A simulated tissue structure composed of these modeling materials will have the same internal field distribution and relative heating functions in the presence of an electromagnetic source as the actual tissue structure. Phantom models of various tissue geometries can be fabricated as shown in Figure 7. They include circular cylindrical structures consisting of synthetic fat, muscle, and bone, and spheres of synthetic brain to simulate various parts of the anatomy. The models are designed to separate along planes perpendicular to the tissue interfaces so that cross-sectional re-

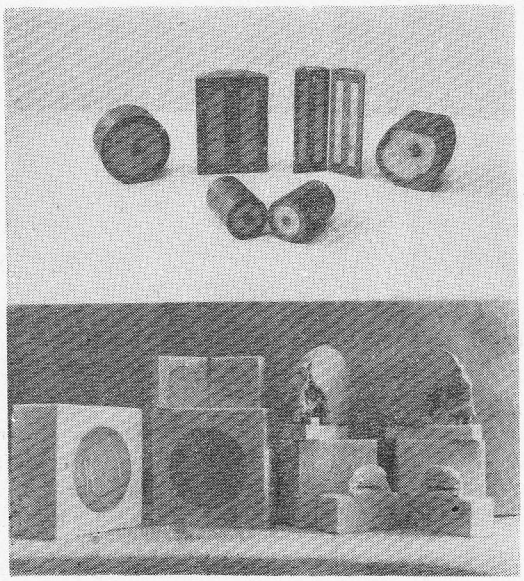

Fig. 7. Phantom tissue models.

lative heating patterns can be measured with a thermograph. A thin (0.0025 cm thick) polyethylene film is placed over the precut surface on each half of the model to prevent evaporation of the wet synthetic tissue. In using the model, it is first exposed to the same source that will be used to expose actual tissue. The power used on the model will be considerably greater, however, in order to heat it in the shortest possible time. After a short exposure, the model is quickly disassembled and the temperature pattern over the surface of separation is observed and recorded by means of a thermograph. The exposure is applied over a 5- to 60-s time interval depending on the source. After a 3- to 5-s delay for separating the two halves of the model, the recording is done within a 5-s time interval, or less. Since the thermal conductivity of the model is low, the difference in measured temperature distribution before and after heating will closely approximate the heating distribution over the flat surface except in regions of high temperature gradient where errors may occur due to appreciable diffusion of heat. The thermograph technique described for use with phantom models can be used on test animals. The animal under test or a different animal of the same species, size, and

characteristics must be sacrificed, however. The sacrificed animal is frozen with dry ice in the same position used for exposure conditions. It is then cast in a block of polyfoam and bisected in a plane parallel to the applied source of radiation used during the experiment. Each half of the animal is then covered with a plastic film and the bisected body is returned to room temperature. The same procedure used on the phantom model is then used with the reassembled animal to obtain absorbed power patterns over the two-dimensional internal surface of the bisected animal. Figure 8 illustrates thermographic recordings taken to assess the absorbed power density in an actual cat head and a 6 cm diameter phantom model of a head. The thermograms at the left of the figure are "C" scans taken over the surface of the separated hemispheres where brightness is proportional to absorbed power and each division is equivalent to 2 cm. The thermograms at the right of the figure are "B" scans taken before and after exposure where spacing between the curves is proportional to absorbed power as a function of vertical distance through the center of each subject. The results clearly show the presence of high absorption areas or "hot spots" in the head of the exposed cat predicted from the theoretical calculations for a sphere. Figure 9 illustrates a thermo-

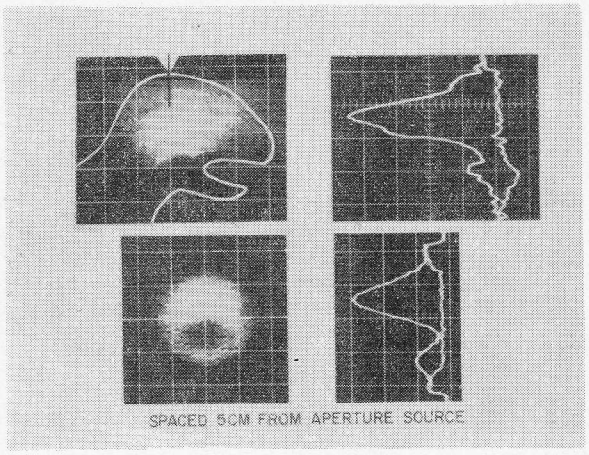

Fig. 8. Comparison between power absorption in cat head and 6 cm diameter phantom sphere (brain tissue) exposed to 918 MHz aperture source as measured with thermograph (peak absorption approximately 0.8 W/kg per mW/cm² incident power).

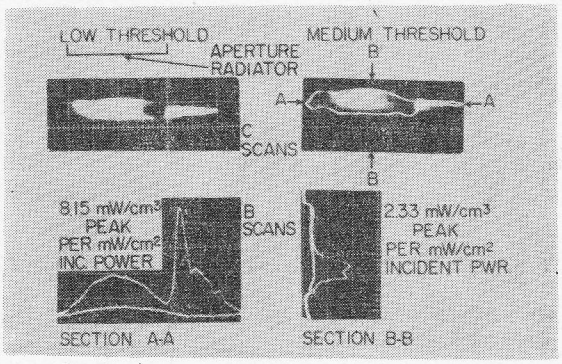

Fig. 9. Thermograms of phantom rat exposed to 918 MHz square aperture source.

WHO - BIOLOGIC EFFECTS & HEALTH HAZARDS OF MICROWAVE RADIATION 1974

graph study made on a phantom tissue model of the body of a rat exposed to a 918 MHz 13 × 13 cm aperture source outlined in the figure. The results clearly illustrate unpredictable absorption peaks (per mW/cm² of incident power) that may occur in the body and tail of the rat. The profound absorption (8.6 mW/cm²) at the base of the tail is due to the increased current density resulting from the sharp change in tissue cross-section. The low absorption in the pelvic area is due to a standing wave null resulting from a body resonance condition, since the rat model is approximately one wavelength long. The results indicate that one must be extremely careful in drawing conclusions from temperature measurements made with rectal thermometers. Also, one cannot make the easy assumption that keeping the tail or any portion of the rat out of the direct beam of radiation will insure non-exposure, and consequently, no absorption. The thermographic technique may be used to detect potential trouble from the use of metal electrodes or thermocouples in exposed biological tissues. Any metal

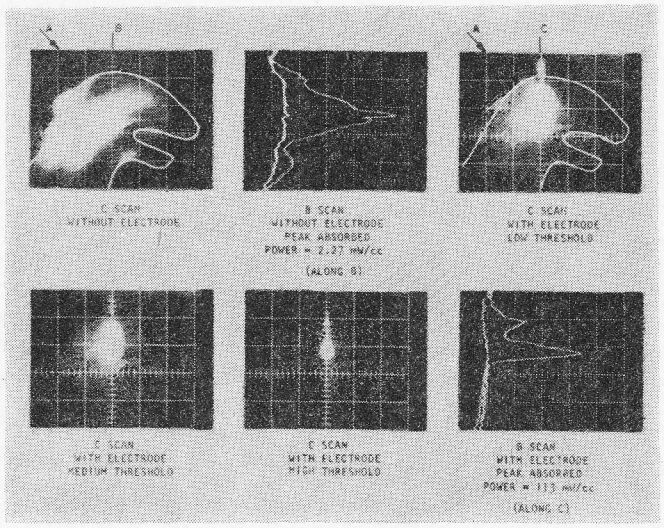

Fig. 10. Thermographic study of effect of coaxial electrode on microwave absorption pattern in the brain of a cat exposed to 918 MHz aperture source (incident power density = 2.5 mW/cm² scale, 1 division = 2 cm).

object placed in tissue can result in serious field distortion and concentration in areas where the object is placed. Figure 10 illustrates thermograms taken of an exposed cat head with and without the presence of a standard coaxial metal electrode used for neurophysiological recordings. The results show a complete shift in the power absorption pattern and two orders of magnitude increase in the absorbed power density in the region where the tip of the probe is located. The past use of such electrodes in assessing the biological effects of microwave radiation on the CNS could result in the interpretation of highly localized thermal effects as non-thermal or low-level effects.

LABORATORY PROTOCOL FOR QUANTIFYING CNS EFFECTS OF EM RADIATION

It is important that any experimental protocol used to quantify absorbed power and associated effects in an animal be carefully planned to eliminate the possibility of misinterpreted data for the various reasons described above. Figure 11 illustrates an ex-

WHO – Biologic effects & health hazards of microwave radiation 1974

perimental protocol used by the author for assessing microwave induced CNS effects. Anesthetized cats are placed in a standard stereotaxic head holder, but the metal ear, orbit, and tooth bars are replaced by plastic parts to eliminate any metallic contact with the cat. The fields are applied to the head with a variable power localized source. The response of the thalamic somatosensory area of the cat's brain to electrical stimulation of the skin on the contralateral forepaw was recorded both with and without the presence of microwave radiation. The gross thalamic electrical response was detected by means of a saline-filled glass electrode with a 60-μm-diameter tip. The electrode was placed in the thalamus and adjusted for optimum thalamic response. The electrode's position was verified in several animals by histologic studies. Metal electrodes were avoided to prevent perturbation of the microwave fields in the brain tissue. The elect-

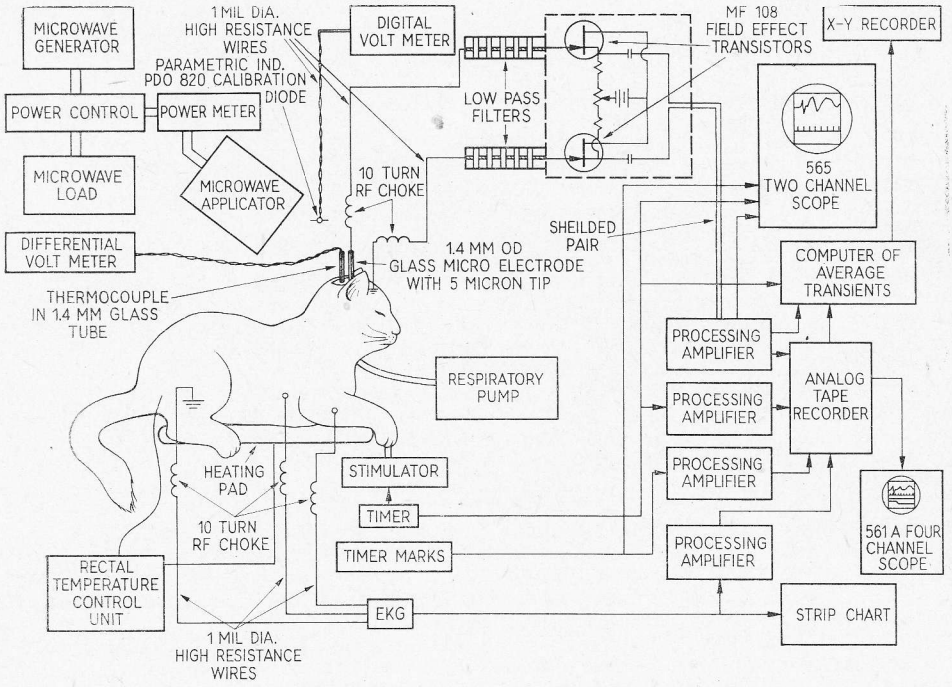

Fig. 11. Block diagram of instrumentation used to quantity CNS effects of microwave radiation in the cat.

rode and associated reference electrodes were coupled to lowpass microwave filters by a pair of 1-mil-diameter[1] high-resistance wires. The filter was designed to provide more than 150-dB attenuation to the microwave with no more than 20 pF of shunt capacitance to the input of a pair of field-effect transistors. The output of the transistors was fed through a processing differential amplifier to an analog tape recorder and computer of average transients. The body temperature of the cat was held constant by a heating pad connected to a rectal temperature control unit. The brain temperature was recorded during the time that the microwaves were off by placing a thermocouple in

[1] 1 mil = 0.001 inch

a glass pipette with a sealed tip at the homologous point in the opposite thalamus (assuming the brain was symmetrical) at the same depth as the recording electrode. The thermocouple was removed during the exposure times to prevent any fringing field effects. The electrical response in the thalamus was recorded continuously with microwaves alternatively on and off in 15-min intervals over a total period of 8 to 12 h. The dosimetry was based on the methods described in the previous section. The EEG response was observed to increase with microwave power density and temperature at much higher levels than that required to produce thalamic changes. The thalamus response characteristics were recorded on an analog tape recorder processed for improved signal-to-noise ratio, both on-line and off-line, by a computer of average transients, and plotted by means of an x—y recorder. The technique was also used to assess evoked responses in other portions of the brain due to audio clicks, light flashes, and incident microwave pulses.

REFERENCES

1. FREY, A. H.: *Science*, 1973, **181**, 356.
2. GUY, A. W., TAYLOR, E. M., ASHLEMAN, B., LIN, J. C.: Microwave Interaction with the Auditory Systems of Humans and Cats. In: *Applications in the 70's. 1973 IEEE G-MTT International Microwave Symposium*. Univ. Col., Boulder, Colo., 1973, p. 321.
3. GUY, A. W.: *IEEE Trans. Microwave Theory Tech.* Special Issue on Biological Effects of Microwaves, 1971, **19**, 205.
4. GUY, A. W., LEHMANN, J. F., STONEBRIDGE, J. S.: Therapeutic Applications of Electromagnetic Power. In: *Special Issue of IEEE Proc.* Industrial, Scientific, and Medical Applications of Microwaves. Jan. 1974 (in press).
5. HUNT, E. L., General Activity of Rats Immediately Following Exposure to 2450 MHz Microwaves. In: *Digest 1972 IMPI Symp.*, Ottawa, Canada, May, 1972.
6. JOHNSON, C. C., GUY, A. W.: *Proc. IEEE* 1972, **60**, 692.
7. JUSTENSON, D. R., KING, N. W.: Behavioral Effects of Low Level Microwave Irradiation in the Closed Space Situation. In: *Biological Effects and Health Implications of Microwave Radiation*. Ed. Cleary, S. F., U. S., Dept. Health, Education, and Welfare. Report BRH/DBE 70—2 (PB 193 858) Rockville, 1969, p. 154.
8. KRAMER, P., EMERY, A. F., GUY, A. W., LIM, J. C.: Theoretical and Experimental Studies of Microwave Induced Cataracts in Rabbits. In: *Applications in the 70's. 1973 IEEE-G-MTT International Microwave Symposium*. Univ. Col., Boulder, Col., 1973, p. 265.
9. LIN, J. C., GUY, A. W., JOHNSON, C. C.: *IEEE Trans. Microwave Theory Tech.* (in press).
10. PHILLIPS, R. D., KING, N. W., HUNT, E. L.: Thermoregulatory Cardiovascular and Metabolic Response of Rats to Single or Repeated Exposures to 2450 MHz Microwaves. In: *1973 Symp. Microwave Power*. Univ. Technology, Loughborough, Sept. 1973.
11. SCHWAN, H. P.: Survey of Microwave Absorption Characteristics of Body Tissues. In: *Proc. 2nd Tri-Serv. Conf. on Biol. Effects of Microwave Energy*, 1958, p. 126.
12. SCHWAN, H. P.: *IEEE Trans. Microwave Theory Tech.* 1971, **19**, 146.

WHO – BIOLOGIC EFFECTS & HEALTH HAZARDS OF MICROWAVE RADIATION 1974

SOME RECENT DEVELOPMENTS IN THE CHARACTERIZATION AND MEASUREMENT OF HAZARDOUS ELECTROMAGNETIC FIELDS

R. R. Bowman

Electromagnetics Division, National Bureau of Standards, Boulder, Colorado, U. S. A.

1. INTRODUCTION

Though some of this paper is relevant to the quantification of fields and energy deposition inside subjects, the discussion will be limited to the measurement of either fields external to subjects or fields unperturbed by subjects.

People and other subjects are often exposed to fields near radiators and in situations where a high level of multipath interference exists. The accurate measurement of such fields has been notoriously difficult. The purpose of this paper is to review briefly some developments over roughly the last five years that have provided some capability for making easy measurements of very complicated fields.

Since this paper is concerned with complicated fields, it is emphasized that the term "electric field strength" is used in the general sense and is defined as the Hermitian magnitude $|E|$ of the field. That is (using rectangular coordinates)

$$|E| \equiv (|E_X|^2 + |E_Y|^2 + |E_Z|^2)^{\frac{1}{2}} \qquad [1]$$

Similarly, magnetic field strength $|H|$ is defined by

$$|H| \equiv (|H_X|^2 + |H_Y|^2 + |H_Z|^2)^{\frac{1}{2}} \qquad [2]$$

Unlike the magnitude $|S|$ of the power density, which is often not a meaningful measure of the intensity of complicated fields, the Hermitian magnitudes are meaningful measures of the strengths of fields having reactive near-field components, multipath components, and arbitrary polarization (9).[1]

2. CHARACTERIZING HAZARDOUS FIELDS

For many years $|S|$ has been used as an index of potential hazards for microwave frequencies (frequencies above 300 MHz). For frequencies below 300 MHz, $|E|$ and $|H|$ are often used (6, pg. 78; 7, pg. 66) rather than $|S|$ mainly because at these lower frequencies: (a) subjects are often exposed to strong reactive near-field components for which $|S|$ is identically zero; (b) it can be important, particularly below 30 MHz, to know both $|E|$ and $|H|$; and (c) available instrumentation uses antennas that

[1] Though $|E|$ is a proper measure of the strength of resonance fields, intense fields with high "Q" may not be hazardous However, reactive near-fields should not be assumed to necessarily have high "Q" values.

measure |E| and |H| separately. (Despite the need to know |H| at some frequencies, the remainder of the paper will be limited to measurements of |E|).

Despite the widespread use of |S| above 300 MHz, it has often been noted that |S| is a poor index of potential hazards even in the microwave band (9); and there is an increasing interest in using |E| or some derived quantity such as $|E|^2$ or electric field energy density $U_E \equiv {}^1/_4 \varepsilon_o |E|^2$. One reason for not using |S| is that intense reactive near-fields can be important for frequencies at least as high as 1 GHz (for example, when subjects are close to or nearly touching leaking cracks). Also, intense standing-wave fields, at any frequency, can have little or no power density. Further, |S| is quite difficult to measure unless one is fortunate enough to be concerned only with stationary, single-component, plane-wave fields with known polarization[2].

Undoubtedly, the recent increase in the use of |E| at microwave frequencies is due to the development of instruments that can measure this quantity with extreme ease[3] over certain frequency ranges despite the presence of reactive near-field components, multipath components, and arbitrary polarization. While there are a number of possibilities for achieving such instrumentation, the author knows of only three types of instruments that have been developed to the degree that they are either advanced prototypes or production models. The latest of these three instrument types are briefly described in the next section[4].

3. RECENTLY DEVELOPED INSTRUMENTS MEASURING |E| IN COMPLICATED FIELDS

3.1. An Instrument Based on a Golay Cell

A broadband, isotropic field sensor was described by Fletcher and Woods (4) in 1969. The sensor is comprised of a pair of thin-walled air-filled spheres connected by tubes to a sensitive differential pressure transducer (see Fig. 1). One sphere is coated with a resistive film that is heated by the EM field to produce a pressure differential between the spheres[5]. The non-coated sphere provides compensation for changes in ambient temperature or pressure. This sensor is essentially a type of Golay cell (5).

---

[2] At sufficiently high frequencies microwave propagation and absorption approximate those of light energy. For these frequencies reactive near-fields are not important with respect to hazards. Also, for multipath fields |S| or |E| measured separately for each component or, perhaps, averaged over the standing-wave variations would likely be better indications of the potential hazards than the maxima of the standing-wave variations. At the present time, the importance of reactive near-fields and standing-waves is not well enough understood to set a definite lower limit on those frequencies for which microwaves can be considered to behave like light waves as far as potential hazards are concerned. Failing definitive information, it seems reasonable that this lower limit should be between 5 GHz and 15 GHz.

[3] Within certain restraints explained later, the instruments are rigorously isotropic in that their response is independent of angular orientation about a given point in complicated fields; and they provide a direct measure of the field level (in various units) without requiring any special technique on the part of the operator.

[4] It is emphasized that the discussions in the following sections should not be interpreted as either endorsements or critiques of the instruments described. Except for the instruments described in Section 3.2, the author has not performed any evaluative measurements on these instruments. The information and data for the instruments described in Sections 3.1 and 3.2 are from the open literature. The reader is cautioned that not all of the important capabilities and limitations of these instruments are discussed in this brief paper. Interpretive comments by the author are believed to be either obvious or easily proven.

[5] Earlier, Schwan (8) had suggested the use of a spherical bulb filled with electrolyte for

WHO – BIOLOGIC EFFECTS & HEALTH HAZARDS OF MICROWAVE RADIATION 1974

Neglecting the perturbing effects of the other parts of the instrument, the symmetry of the energy-absorbing sphere insures that the response of the sensor will be independent of its angular orientation in fields of arbitrary complexity. Further, for wavelengths much longer than the diameter of the sphere and if the surface resistivity of the sphere is large enough, the response of the sensor will be determined to a good approximation solely by the value of $|E|^2$ at the position of the sensor regardless of the configuration of the field[6]. To the author's knowledge, the response of this type

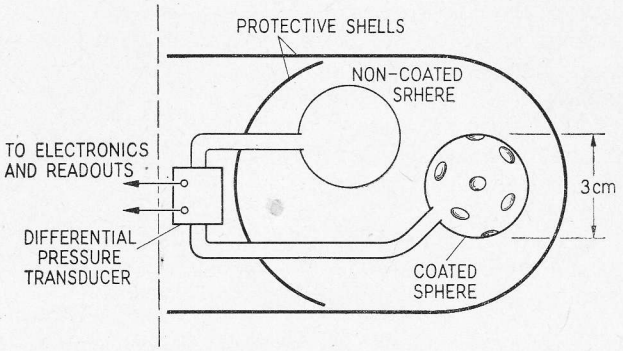

Fig. 1. Schematic representation of a wideband, isotropic field sensor. The field sensing sphere is coated with a high-resistivity film. The spots are regions of lower resistivity that provide an extended upper frequency response. The protective shells prevent temperature differences between the spheres due to either air currents or radiations above the microwave region.

of sensor has not been established for arbitrary fields with wavelengths comparable with or shorter than the sphere diameter. (The issue is: what kind of average of $|E|^2$ will the sensor provide for standing-wave fields or reactive near-fields that have large electric field gradients over the sphere?) However, it has been shown that the sensor will have an essentially constant response for single plane-wave fields with wavelengths either long or short compared with the sphere (10).

An instrument using this type of sensor was marketed[7]. Some of its important characteristics are listed in Table 1. Some other important characteristics and limitations are discussed here. An important capability of the sensor is that it can be expected to accurately sum the intensities of multifrequency fields. A serious limitation is its slow response time of about 20 seconds (90 percent). Also, the sensitivity is rather limited, but perhaps further development could improve this limitation. The sensor can withstand fields of 1 watt/cm^2 average level (4), but the peak intensity overload is apparently not known.

---

a field sensor, but apparently the slow rate of temperature rise of the electrolyte prevented a practical application of this type of sensor except for laboratory use.

[6] For long wavelengths the unperturbed electric field will be essentially uniform over the sphere for any field configuration. The currents in the coating when the sphere is introduced into the field will be due to the final tangential field over the sphere; and, for a large surface resistivity, the final tangential field will not differ significantly from the unperturbed field. Thus, the response of the sensor, to a good approximation, will not be affected by the magnetic field and the sensor will have the same response coefficient for $|E|^2$ in a reactive near-field or standing-wave field as it would for a simple plane-wave field.

[7] By the Wayne Kerr Company Limited, New Malden, Surrey, England. For reasons unknown to the author, it was subsequently removed from the market.

WHO – Biologic effects & health hazards of microwave radiation 1974

Table 1

Table of instrument characteristics

For instruments described in:		Section 3.1	Section 3.2	Section 3.3
Frequency range (GHz) for ± 1 dB response for single plane-waves		0.4 to 40	0.03 to 3[1]	0.85 to 15
Upper frequency (GHz) limit for spatial resolution of complicated fields.[2]		1.25	4.7	1.1
Field levels measurable[3]	Field strength $\lvert E \rvert \left(\frac{V}{cm}\right)$	0.34 to 3.4	0.009 to 47.5	0.09 to 6.1
	Equivalent plane-wave $\lvert S \rvert \left(\frac{mW}{cm^2}\right)$	0.3 to 30[4]	0.0002 to 6000[5]	0.02 to 100[6]

1. Can be extended to about 5 GHz by using a different detector-diode package.
2. These limits are somewhat arbitrarily chosen. They correspond to a wavelength for which the sensor dimensions are approximately 1/8 wavelength.
3. All three instruments respond essentially to $\lvert E \rvert^2$, but they are calibrated to read in different units. For purposes of comparison, their capabilities have been stated here in terms of $\lvert E \rvert$ and in terms of the power density in a simple plane-wave field with corresponding $\lvert E \rvert$.
4. Using only one probe.
5. Using three probes. Any single probe covers a dynamic range of 40 to 50 dB depending on the choice of input amplifier.
6. Using two probes. Each probe covers a dynamic range of 20 to 30 dB depending on the choice of input amplifier.

Note: some minor approximations have been made in order to simplify the comparisons in this table

3.2. An Instrument Based on Three Orthogonal Dipoles

A second type of broad-band, isotropic field sensor was described by Bowman, Larson, and Belsher in 1970 (2, 3). This type of sensor consists of three orthogonal dipoles with diode detectors connected between the arms of the dipoles. Each diode is separately connected to signal processing circuitry by a pair of high-resistance leads (see Fig. 4). The high resistance leads cause little perturbation of the field being measured and also provide powerful filtering so that only the DC value of the rectified signal at the diode is conducted to the electronics. For low intensity fields, and assuming wavelengths long compared to the dipoles, the detected signals from the orthogonal elements of the field sensor are proportional to the square of the corresponding electric field components. After equalizing the responses of the three channels, the summing amplifier output is proportional to $\lvert E \rvert^2$. For higher intensity fields, the non-linear characteristics of the summing amplifier provide extended dynamic range. The readout of the instrument is calibrated to display $^1/_4\varepsilon_o \lvert E \rvert^2$. For wavelengths up to perhaps two or three times the length (8 mm) of the dipoles, the probe can be calibrated to measure single plane-wave fields (or to provide some sort of average reading for multipath fields). The response of the probe will, of course, be much greater in the resonance region for the dipole.

Since orthogonal dipoles with common centers do not mutually couple, early models of this type of sensor placed the dipoles so that they had a common center. How-

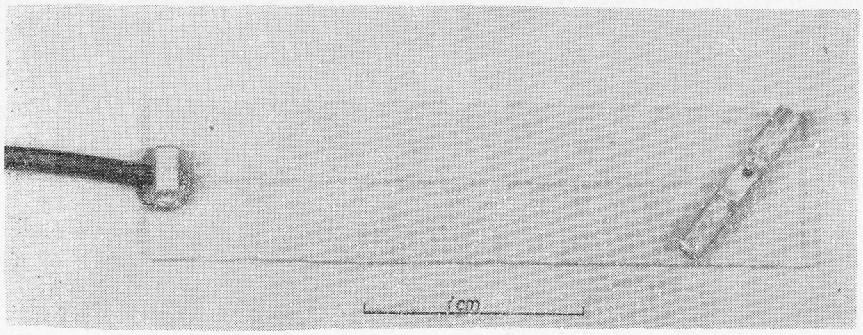

Fig. 2. Photograph of one of three identical elements that are fitted together to form a sensor with three orthogonal dipole-diode field detectors. The deposited thin-nichrome films on the substrate form a balanced twin-lead with linear resistances of about 50 kΩ/cm. The high-resistance twin-leads connected to the rear of the substrate are made of carbon-loaded Teflon and have a linear resistance of about 3 to 30 kΩ/cm (depending on the instrument model).

ever, this arrangement tends to maximize the "cross-talk" between the three pairs of high-resistance lines near the common center where significant, though small, differential-mode radiofrequency currents exist on these lines. Present models utilize the fact that the dipoles can be displaced from center without introducing a serious amount of coupling between the dipoles. Figure 2 shows one of three identical elements consisting of a dipole, diode, and deposited nichrome thin-film resistance lines, all located on a substrate. The acute angle between the dipole and the high-resistance leads is

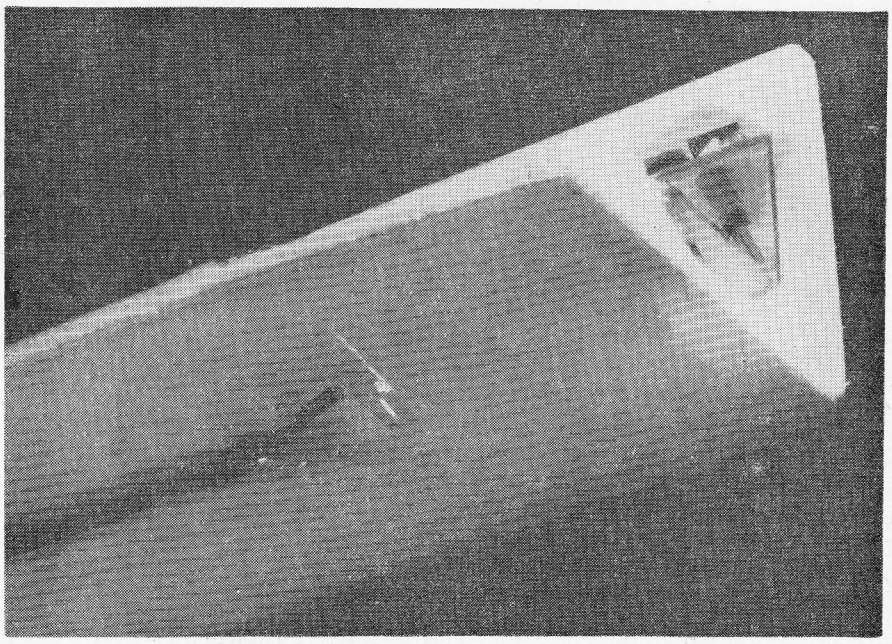

Fig. 3. Photograph of the field sensor assembled inside a low-density polyfoam support. The three identical elements (see Fig. 2) are fitted together to form a triangular cross section tube.

WHO – BIOLOGIC EFFECTS & HEALTH HAZARDS OF MICROWAVE RADIATION 1974

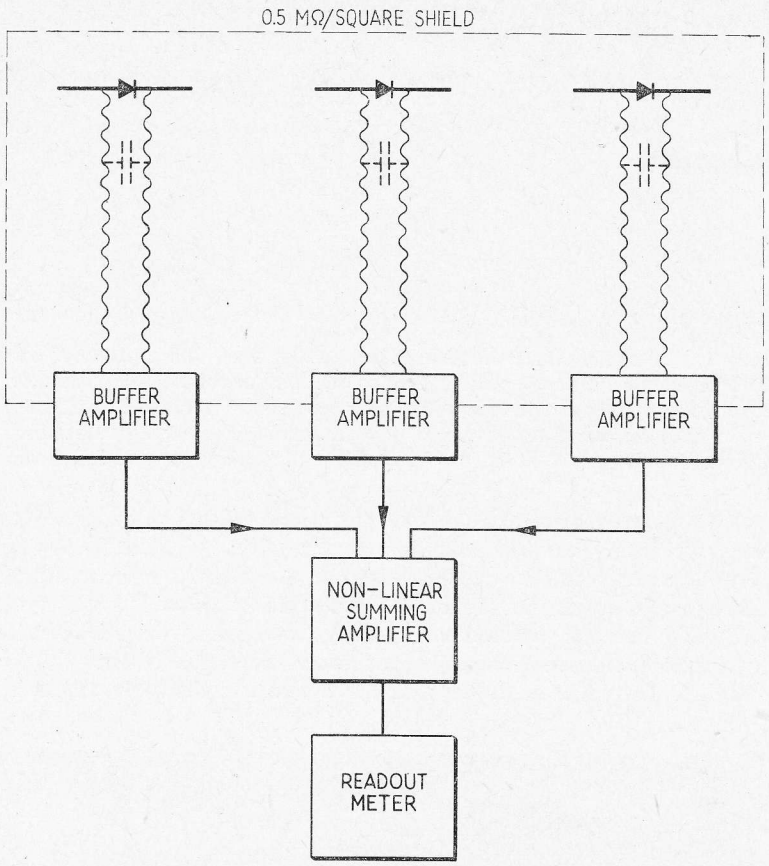

Fig. 4. Functional representation of the instrument described in Section 3.2. The dipole-diode field detectors are located at the end of a wand and the buffer amplifiers are located in the handle of the wand. (See also Fig. 5). The non-linear summing amplifier and readout electronics are connected to the wand by a cable (which can be 20 meters or more in length). Each probe channel can be read separately for test purposes and to determine the orthogonal components of the (electric) field.

54.74 degrees. This angle provides orthogonality between the dipoles when the three elements are placed together along the long edges to form a tube with an equilateral triangle for a cross-section. Figure 3 shows this tube inserted into a hole drilled in the end of a polyfoam support. The high-resistance lines connecting the elements to the electronics are made from carbon-loaded Teflon and can be almost any length desired. The polyfoam support is fitted snugly inside a thin-walled plastic tube (see Fig. 5) for protection. To reduce "capacitive" current noises in the high-resistance lines, the protective tube is coated with a slightly conductive layer which is bonded to the metal handle of the probe with silver-conductive glue.

As shown in Table 1, an important characteristic of this instrument is its sensitivity. It is the only instrument described here that is sensitive enough to measure the low intensity fields of interest to some countries. However, it must be emphasized that the present designs will provide accurate readings only for fields that do not have mo-

WHO - Biologic effects & health hazards of microwave radiation 1974

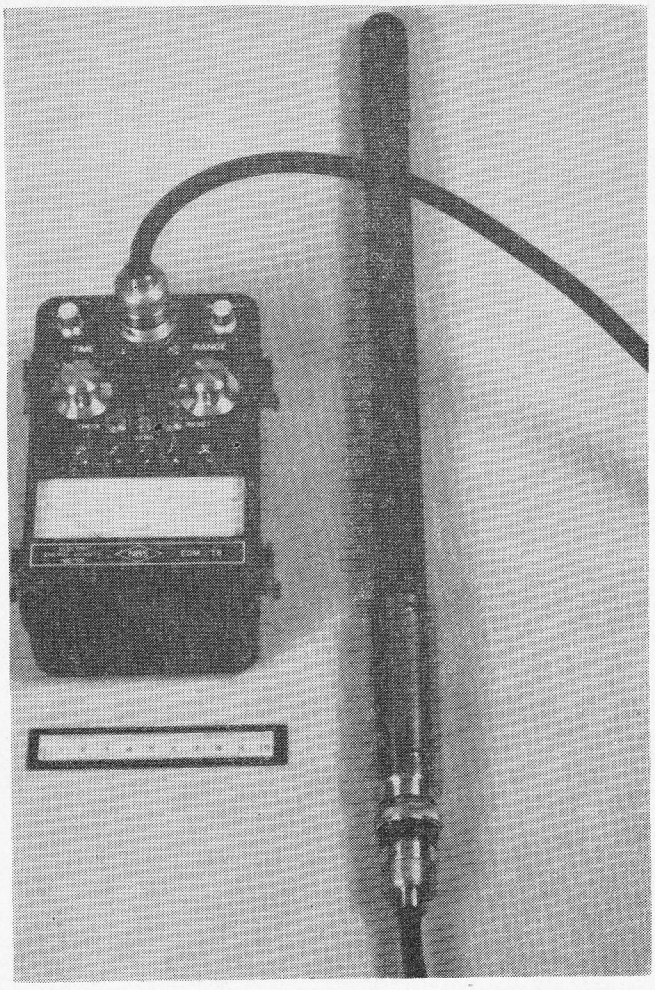

Fig. 5. Photograph of the instrument described in Section 3.2. The probe shown here is short (about 0.5 meters). For measuring fields at the lower end of the microwave band or below, the field sensor can be located in a wand 3 meters or more in length. The handle of the probe is metal and a high-resistance shield extends on the outside of the wand, providing a continuous shield for the probe to prevent "quasistatic" noise.

dulations that exceed the bandpass (approximately 0 to 3000 Hz) of the probes[8]. Another limitation of the instrument is that it will not accurately measure multifrequency fields. In multifrequency fields the instrument tends to read "high", but the error will not be greater than 3 dB if only two intense fields are present. Typically, the probes will withstand continuous wavefield intensities at least 10 dB greater than the highest measurable level. The peak intensity overload is not presently known.

[8] Probes are under development that will read peak field levels for fields with repetitive wave forms, even fields with sub-microsecond rise-times.

WHO – Biologic effects & health hazards of microwave radiation 1974

3.3. An Instrument Based on Lossy Elements Made from Thin-Film Thermocouples

A publication by Aslan in 1972 (1) described another isotropic, wide-band field sensor. This field sensor is composed of three orthogonal lossy elements (see Fig. 7) that are heated by the field. Each element consists of a series of thin-film thermocouples (see Fig. 6) deposited on a plastic substrate. Assuming that the wavelength is long compared with the length (about 3 to 4 cm) of the thermocouple strips, and since the linear resistance of the strips is high enough to cause only slight field perturbations, the heating in each strip is directly proportional to the square of the original electric field component along it. The thermocouples provide a signal proportional to the heating, and the three outputs from the elements are conducted along high-resistance leads and then summed to provide a signal proportional to $|E|^2$. However, the instrument (see Fig. 8) is calibrated to read in units of mW/cm^2.

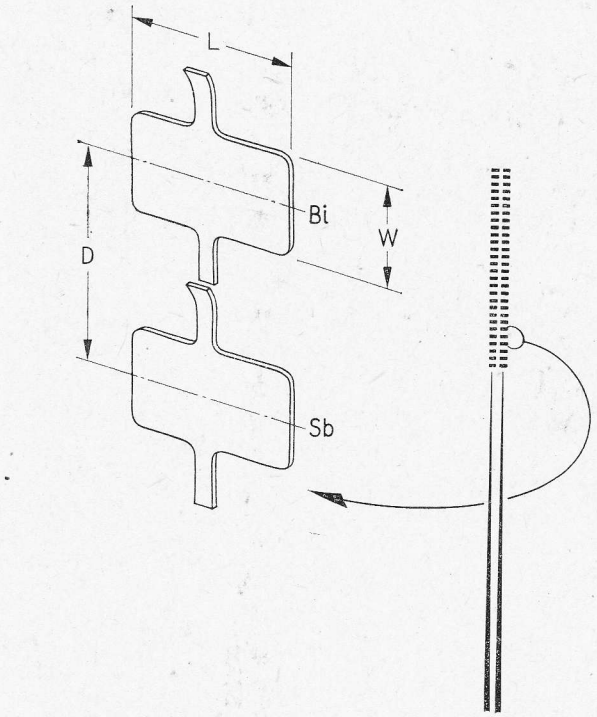

Fig. 6. Field sensor element with distributed thin-film resistive thermocouples (Antimony-Bismuth). Tapered resistive-film leads reduce interaction between leads and elements. Owing to the higher resistance of the narrow portions of the elements, most of the heating occurs there. The broad portions of the elements provide a heat sink to the ambient air. Three elements are orthogonally arranged as shown in Fig. 7.

Referring again to Figure 6, nearly all of the heating occurs in the narrow portions of the thermocouples. The wide portions provide "heat sinks" to the substrate and to the ambient air. This arrangement provides a low ambient-temperature sensitivity (less than 0.05 percent C).

For single plane-wave fields the type of sensor described above has an essentially constant response coefficient for a wide range of wavelengths both larger and smaller than

WHO – BIOLOGIC EFFECTS & HEALTH HAZARDS OF MICROWAVE RADIATION 1974

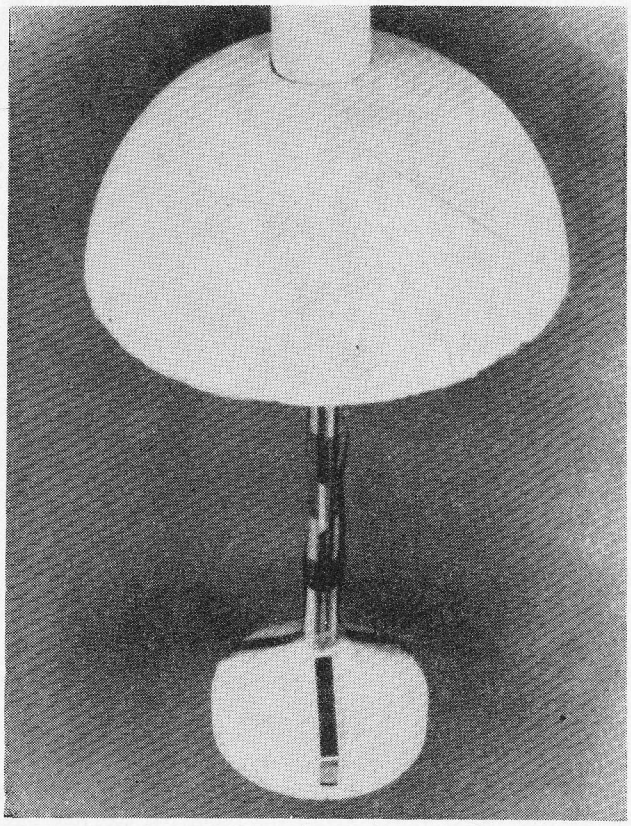

Fig. 7. Internal view of the probe. Three field sensing elements (see Fig. 6) are arranged orthogonally on a low-density polyfoam support. The support is located inside a 10 cm diameter low-density polyfoam sphere.

the lengths of the elements. For complicated fields one would expect that the sensor would provide some sort of average of $|E|^2$ over, roughly, the volume of a sphere circumscribing the sensor. However, it has not been shown, to the author's knowledge, that this average would be the simple average of $|E|^2$. In fact, it is easy to show that the sensor can give a zero reading when the average of $|E|^2$ is not zero[9]. This limitation may not be very serious since a reasonable indication of the average strength of the field can probably be obtained as the probe is moved throughout the field region of interest.

[9] Imagine a standing-wave field composed of two travelling waves of equal magnitude and opposite directions. Assume a wavelength smaller than the length of the elements of the sensor so that the multipath field will have strong gradients within the volume of the sensor. If the sensor is oriented so that the apex of the orthogonal elements is at a point of zero field strength and one of the elements is parallel to the electric field direction, the output of that element will be zero. Since the other two elements will be orthogonal to the electric field their outputs will also be zero. Thus, the instrument reading will be zero even though the average of $|E|^2$ could be very large over the volume of the sensor. Further, the response of the sensor will not be independent of its angular orientation at the field point.

WHO – BIOLOGIC EFFECTS & HEALTH HAZARDS OF MICROWAVE RADIATION 1974

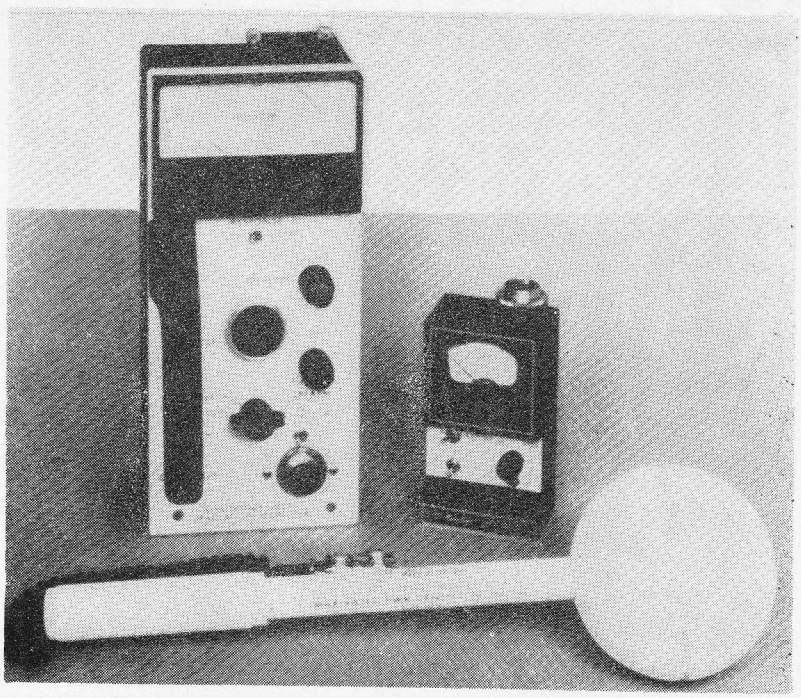

Fig. 8. Photograph of the instrument described in Section 3.3. The larger electronics unit provides additional features such as recorder output and audible alarm.

As shown in Table 1 this instrument has fairly good sensitivity[10]. It has rather limited capability to resolve intensity variations in the field, but perhaps this limitation can be reduced with further development. The instrument can accurately measure multi-frequency fields. The overload for continuous wave fields is 100 to 300 mW/cm² and the peak overload is 20 to 60 watts/cm², depending on the probe model.

4. CONCLUDING REMARKS

The need to measure easily very complicated fields for the evaluation and control of hazardous emissions has resulted in several instruments that have considerable capability for this difficult measurement task. Though they all have serious limitations, these, and other, instruments are still evolving rapidly. It is reasonable to believe that instrumentation will soon be available to permit easy measurements for nearly all hazardous emissions of interest.

REFERENCES

1. ASLAN E.: *IEEE Trans. on Instrumentation and Measurement*, 1972, **IM-21**, 4, 421 (November).
2. BOWMAN R. R., LARSEN E. B., BELSHER D. R., WACKER P. F.: Second progress report. *Electromagnetic hazards project, unpublished NBS Report*, 1970 (September).

[10] An instrument of this type has been marketed by the Narda Microwave Corporation, Plainview, New York, U. S. A.

3. BOWMAN R. R.: *An isotropic electric energy-density probe for high-level fields,* presented at Internat. Union Radio Science, Spring Meeting, Washington, D. C., April 8—10, 1971.
4. FLETCHER K., WOODS D.: *Thin-film spherical bolometer for measurement of hazardous field intensities from 400 MHz to 40 GHz,* Non-Ionizing Radiation, 57, 1969 (September).
5. GOLAY M. J. E.: *Rev. Sci. Instr.,* 1949, **20**, 816 (November).
6. MARHA K., MUSIL J., TUHÁ H.: *Electromagnetic Fields and the Life Environment.* San Francisco Press, Inc., 1971.
7. PRESMAN A. S.: *Electromagnetic Fields and Life,* F. A. Brown, Jr. Ed. New York — London: Plenum, 1970.
8. SCHWAN H. P., Electrical Substituties for Human Tissue. In: *Proc. Third Annual Triservice Conference on Biological Effects of Microwave Radiating Equipment,* 1959.
9. WACKER P. F., BOWMAN R. R.: *IEEE Trans. on Microwave Theory and Techniques,* 1971, **MTT-19**, 2, 178 (February).
10. WILLIAMS W. E.: *Proc. IEE,* 1970, **117**, 12, 2236 (December).

WHO – BIOLOGIC EFFECTS & HEALTH HAZARDS OF MICROWAVE RADIATION 1974

METHODS OF CALIBRATING MICROWAVE HAZARD METERS

R. C. Baird

Electromagnetics Division, National Bureau of Standards, Boulder, Colorado, U. S. A.

INTRODUCTION

Accurate and reliable measurements of microwave radiation are required for hazard surveys, leakage detection, testing of products for compliance with regulations, and for determining exposure levels in experiments designed to investigate the biologic effects of microwave radiation. Accurate calibration of the instruments used for these measurements is essential for safety reasons and to provide a basis for comparison of the experimental results of various laboratories.

Existing calibration methods require that a known field intensity be established through measurement, calculation, or a combination of both. The device under test is placed in the "standard" field and the meter indication is compared with the known field value. This paper describes three different approaches to the problem of producing the "standard" calibrating field: 1) the free-space standard field method, 2) guided wave methods, and 3) the standard probe method. The first method is discussed in somewhat more detail than the other two because it is presently more widely used. Due to space limitations, all discussions are limited to descriptions of the basic concepts, the advantages and limitations, and estimates of the accuracies attainable with each method. An effort was made to include references adequate to enable interested persons to fill in the details. This was not always possible because some recent work has not been published and there are some problems that need further investigation.

FREE-SPACE STANDARD FIELD METHOD

There are several variations of this method, but the objective is always to establish a known calibrating field in free space. The most common experimental arrangement is shown in Figure 1. The power density $|S|$ at a point on the transmitting axis at a distance d from the transmitting antenna is given by

$$|S| = \frac{P_T G}{4\pi d^2} \qquad [1]$$

where P_T is the net power delivered to the transmitting antenna, and G is the effective gain of the transmitting antenna. The gain is normally determined in advance, and P_T and d are measured as part of the regular calibration procedure.

The most convenient method of determining P_T is by means of a dual directional coupler as indicated in Figure 1. The incident power P_i and the reflected power P_r are monitored with the coupler sidearms, and P_T is obtained from the relation $P_T = P_i - P_r$. High quality, broad-band couplers are available, along with methods for

WHO – BIOLOGIC EFFECTS & HEALTH HAZARDS OF MICROWAVE RADIATION
1974

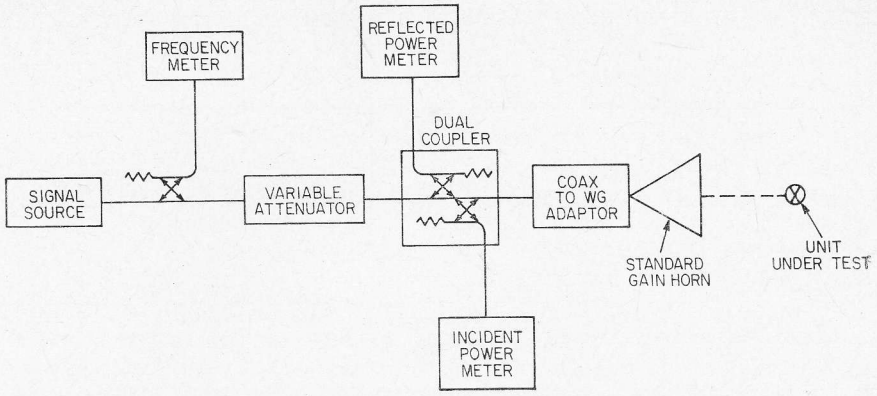

Fig. 1. Diagram of the basic experimental arrangement required for the free-space standard field method.

using them to determine P_T (4, 8, 9, 10). The methods cited are for calibrating power meters but the same techniques can be applied to antennas. The coupler described in (10) can be used from 0.3 to 8.5 GHz to determine P_T to within 1 or 2 percent* if corrections are made for mismatch effects. The foregoing assumes that the device being calibrated is sufficiently small and far enough away that the amount of energy reflected back into the transmitting system is insignificant. If this condition cannot be met, it is possible to obtain a correction for the effect of the reflected energy by varying d, observing the (approximately) sinusoidal variations in P_r, and then averaging P_r over at least one full cycle.

The principal sources of error in this method are uncertainties in the gain determination and multipath interference. Multipath effects are often overlooked, but every calibrating facility will have some scattering associated with it which may cause the field in the calibrating region to be significantly different from that predicted by equation 1. Even high-quality anechoic chambers are not perfect and, in fact, they are often worse than the user is led to believe. It is difficult to adequately evaluate this error and a treatment of the subject is beyond the scope of this paper. A useful discussion of the problem is given by Bowman (2).

When the multipath and gain problems are combined, one is indeed faced with a dilemma. The most accurate gain values are obtained for large distances, but large distances require greater transmitter power and the multipath situation is worse. On the other hand, there are some fundamental difficulties associated with accurate gain determinations at short distances. It will be instructive to take a closer look at these problems, particularly as they relate to so-called "standard gain horns". These pyramidal horns are commonly employed as radiators because they are rugged, stable, cover a relatively broad frequency band, and the problem of determining their gain has received a lot of attention.

The effective gain G of any antenna is a function of distance and approaches a constant G_o as d approaches infinity. This is illustrated in Figure 2 which shows the estimated gain reduction for a representative example (13) plotted as a function of the parameter $n = d\lambda/a^2$, where a is the largest aperture dimension and λ is the free space

* The uncertainties stated here are intended to include all known, significant sources of error and correspond roughly to 95 percent confidence limits. However, uncertainties quoted from the published literature should be interpreted as indicated in the original article.

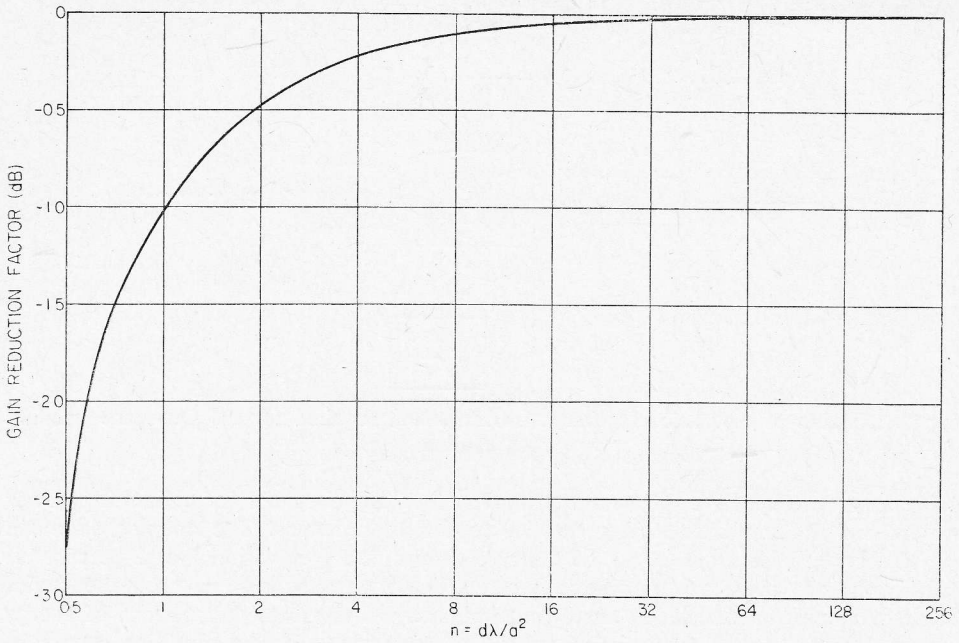

Fig. 2. Estimated near-field gain reduction for a pyramidal horn based on the method of Jull (13).

wavelength. In establishing a calibrating field, one must use the correct value of G for the specific distance involved; otherwise significant errors can result. The far-field gain G_o can be calculated to sufficient accuracy ($\approx$ 0.3 dB) for many purposes (5, 11, 13, 16, 18) and may be measured to within about 0.1 dB if necessary (2, 6, 12, 14, 15, 19, 20). The values of G_o obtained by these methods hold for $d >> a^2/\lambda$ (i.e., large n values). For distances greater than about one or two a^2/λ, it may also be possible to calculate G to within about 0.3 dB for pyramidal horns (13). However, the accuracy of these near-zone calculations has not been definitely established.

There are also problems in experimentally determining the near-field gain. The usual gain measurement approach involves measuring the power transmitted between a pair of antennas and applying the equation

$$G_T G_R = \frac{P_R}{P_T}\left(\frac{4\pi d}{\lambda}\right)^2 \qquad [2]$$

where P_R is the received power, G_T and G_R are the gains of the transmitting and receiving antennas, respectively, and d is the distance between the antennas. Equation [2] holds rigorously only in the far field. At shorter distances, G_T and G_R cannot be separated into the individual factors (19). Since one can always measure P_R/P_T, it is tempting to apply equation [2] to the case of two identical antennas in the near-field and obtain $G_a^2 = (P_R/P_T)(4\pi d/\lambda)^2$, where G_a is the measured apparent near-field gain of the two antennas. However, G_a obtained in this manner is not the correct near-field gain. In other words, G_a will not give the correct on-axis power density when used in equation [1]. This can perhaps be seen intuitively. P_R is the result of an integration (or averaging) of the incident field distribution over the receiving aperture, and unless the incident field is a plane wave, there is no simple relationship between G_a

WHO – Biologic effects & health hazards of microwave radiation 1974

and the desired on-axis power density. The error will, of course, increase as d becomes smaller.

This problem can be partially overcome in at least two ways.

1. If one antenna is small (an open-ended waveguide for example) and its far-field gain is known, it can be used to measure the on-axis gain of a larger antenna at relatively short distances. The measurements should be reasonably accurate ($\simeq$ 0.5 dB) so long as d is greater than about eight a^2/λ for the small antenna and more than one or two a^2/λ for the large antenna. The dimensions of the probe being calibrated should also be less than the aperture dimensions of the small antenna. This procedure was followed by Woods (21) who claims an overall uncertainty in the calibrating field of $\pm$ 0.5 dB from 1 GHz to 18 GHz and $\pm$ 1 dB up to 35 GHz.

2. When it is necessary to calibrate large numbers of nominally identical hazard meters, the extrapolation method described in (15) is particularly useful when applied as follows. Let B_d be the meter indication with the probe at an arbitrary near-field distance d, and B_o the indication with the probe at a large distance d_o where far-field conditions hold. We can write the relations where $|S|_o$ is the far-field power density, $|S|_d$ is the equivalent plane-wave power density in the near-field, and K is

$$B_o = K|S|_o, \quad B_d = K|S|_d, \tag{3}$$

a proportionality factor which relates the meter indication to the incident power density. In the extrapolation technique, B_d is measured over a range of distances and a power series is fitted to the product $B_d d^2$ over the measurement interval. This series is then used to determine $B_o d_o^2$ by extrapolation. One can then obtain the ratio

$$\frac{B_d d^2}{B_o d_o^2} = F_d \tag{4}$$

Substituting for B_d and B_o from equation [3], we obtain

$$|S|_d = F_d S_o \left(\frac{d_o}{d}\right)^2 = \frac{F_d P_T R_T}{4\pi d^2} \tag{5}$$

since $|S|_o = P_T G_T/(4\pi d_o^2)$. P_T can be measured, and G_T (the far-field gain of the transmitting antenna) can be obtained by the extrapolation method or other methods previously referred to. The near-field correction factor F_d is a function of d, and must be determined for every combination of radiator and type of probe. However, once F_d has been obtained for a given probe, it can be used to calibrate other probes of the same type with little additional error.

It should be pointed out that, for rectangular apertures

$$|S| \simeq \frac{\varepsilon P_T}{n^2 A_p}\left(\frac{b}{a}\right)^2 \tag{6}$$

where ε is the aperture efficiency, $A_p = ab$ is the physical area of the aperture, and a and b are the aperture dimensions (a being the largest). For horns of a given design, the ratio b/a and ε are approximately constant, so the power density for a particular value of n is inversely proportional to the aperture area. It is desirable to have n as large as possible to reduce the gain uncertainty; therefore, if P_T is limited, it is necessary to use smaller apertures in order to achieve the required calibrating field intensity.

At the National Bureau of Standards we presently use standard horns above 2.6 GHz to establish 10 mW/cm² fields to an accuracy of $\pm$ 0.5 dB, including multipath effects. The required transmitter power is only 10 to 20 watts. Below 2.6 GHz we use an open-ended waveguide as the radiating element. The gain calculations for horns do not

give accurate results for the waveguide, so the gains are measured by the techniques described in (15). Present accuracy down to 0.9 GHz is ± 0.6 dB. Transmitter powers of 35 watts or less are required to produce a 10 mW/cm² field. We believe open-ended guides can be used down to about 0.3 GHz and are in the process of determining the accuracy of this method over the 0.3 to 0.9 GHz range.

GUIDED WAVE METHODS

The fields inside a waveguide can be accurately calculated and, in some cases, are sufficiently uniform to be considered for calibration purposes. The main advantage of such a system is that considerably less power and space are required. One disadvantage is that the maximum transverse dimensions of the structure must be less than $\lambda/2$ for the highest calibration frequency in order to avoid higher order modes which result in complicated field distributions. Hence, the method is only useful for frequencies below 1 or 2 GHz, since the device being calibrated must be small compared to the guide dimensions.

Figure 3 shows how a section of a rectangular waveguide can be used for calibrations. A reflectionless load is connected to the output end to prevent standing waves which would cause serious errors in the calibration. The probe to be calibrated is inserted

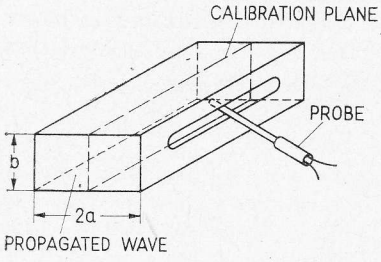

Fig. 3. A section of rectangular waveguide modified for use as part of a probe calibration system.

into the waveguide through a hole in either the top or side wall and positioned in the center of the guide where the field is most nearly uniform. The access holes should be as small as possible. Equations for calculating the field distribution from P_n (the net power delivered to the section) and the guide dimensions can be found in any book on waveguide theory. P_n is determined in the same way as P_T in equation [1].

It is difficult to estimate the total uncertainty of this method because the field intensity will be modified by the size and nature of the probe being calibrated. Woods (21) describes a system which operates from 400 to 600 MHz with an estimated uncertainty in the field intensity of ± 12 percent. Aslan (1) uses a waveguide set-up at 2450 MHz which he believes is accurate to within ± 6 or 7 percent, based on comparisons with free-space measurements using a standard gain horn.

An example of a different type of guided wave structure which has been used at the National Bureau of Standards is illustrated in Figure 4. The basic unit is a section of two-conductor transmission line operating in the transverse electromagnetic mode (TEM), hence we call it a TEM Transmission Cell. As shown in the Figure, the main body of the cell consists of a rectangular outer conductor and a flat center conductor located midway between the top and bottom walls. The dimensions of the main section and the tapered ends of the cell are chosen to provide a 50-ohm impedance along the entire length of the cell — see (7, 17) for some design information. When the cell is carefully made and terminated in a reflectionless load, the input VSWR is usually less than 1.05 and always less than 1.1 for all frequencies below the cut-off limit. The field

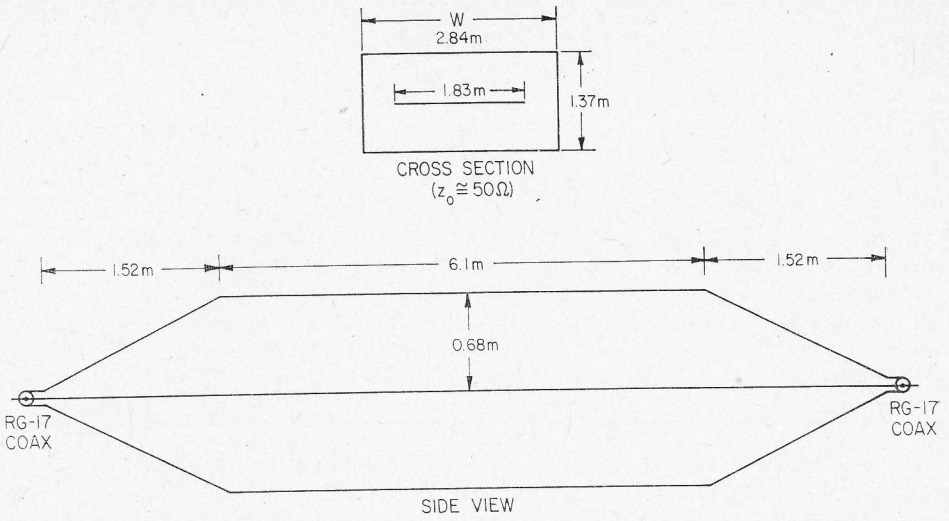

Fig. 4. A type of TEM Transmission Cell used at the NBS for calibrating hazard meters and for measuring susceptibility of electronic equipment to EM fields. These cells can also be used as exposure chambers for studying biologic effects.

intensity in the center of the cell can be quite uniform as shown in Figures 5 and 6, and the wave impedance throughout the cell is very close to the free-space wave impedance as shown in Figure 7. These features are the principal reasons for using this type of cell for calibrations.

The E-field in the center of the cell, half way between the center conductor and the top (or bottom) wall, will be vertically polarized and is given by

$$E_V = \frac{\sqrt{P_n R_c}}{d}, \qquad [7]$$

where R_c is the real part of the characteristic impedance of the cell, and d is the distance from the upper wall to the center plate. P_n (the net power delivered to the cell)

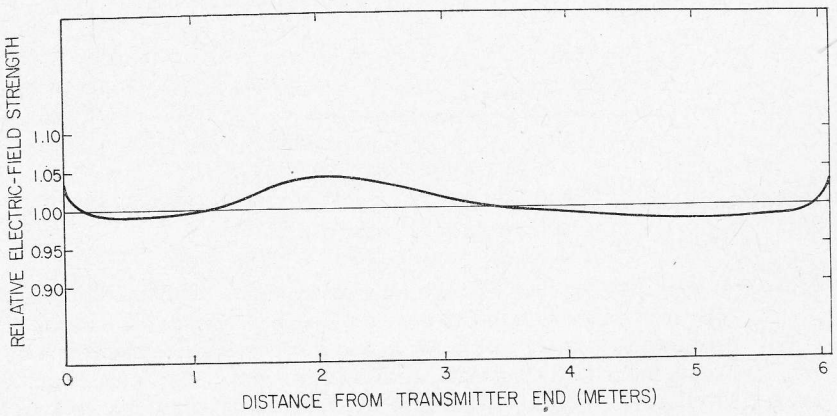

Fig. 5. Relative longitudinal E-field distribution of TEM Cell measured along the center line of the cell 30 centimeters above the center strip.

WHO – Biologic effects & health hazards of microwave radiation
1974

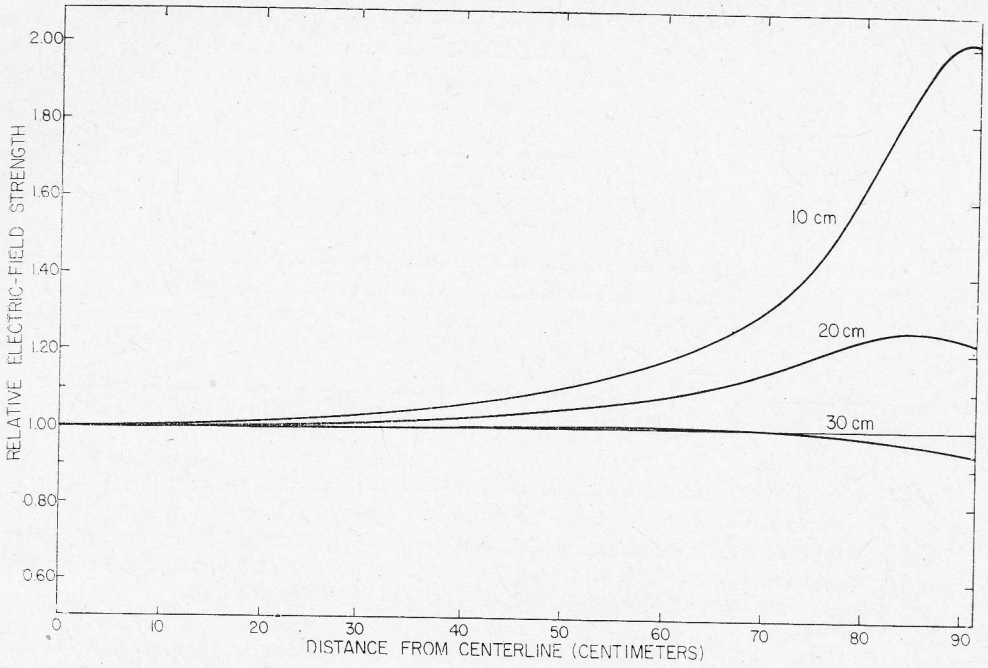

Fig. 6. Relative E-field distribution of TEM Cell measured in a transverse plane midway between the ends at three heights above the centerstrip.

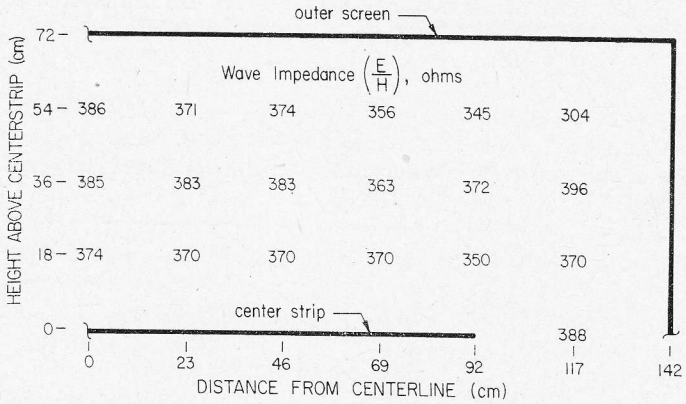

Fig. 7. Calculated values of wave impedance for the TEM Cell in a transverse plane midway between the two tapered ends.

is determined in the same way as P_T. We have used a time-domain reflectometer to determine R_c. The introduction of the probe into the test region will change R_c and alter the field distribution slightly, but if the probe is much smaller than the transverse cell dimensions, this error will be small. Although we have not fully evaluated the errors associated with this method, we believe the total uncertainty can be kept below $\pm$ 1 dB. We have used these cells to generate fields of 10 V/m to 500V/m from dc to 600 MHz, but a practical upper frequency limit for accurate calibrations may be somewhat

WHO – Biologic effects & health hazards of microwave radiation 1974

lower ($\approx$ 500 MHz), depending on the size of the device to be calibrated. The cells can be made in various sizes to suit particular needs, but the width (W in Fig. 4) must be less than $\lambda/2$ at the highest design frequency.

STANDARD PROBE METHOD

This method is the simplest, and it may ultimately prove to be the best method of calibrating hazard meters for general use. The idea is to have a stable and reliable probe that has been accurately calibrated and use it as a "transfer standard". That is, the standard probe would be used to determine the field intensity over a particular region in space (or in a guided system) produced by an arbitrary transmitting antenna. The probe to be calibrated would then be placed in the same location in the field and the meter reading compared with the known value of the field. The only requirements on the transmitter are that it generate a field which has the desired magnitude, is constant in time, and is sufficiently uniform over the calibrating region.

A dipole-diode probe of the type developed by Bowman (3) can probably be improved to the point where it could serve as such a transfer standard. These probes have a nearly isotropic response pattern and a large dynamic range ($\geq$ 40 dB); they are rugged, practically burn-out proof, can be made very small (1 or 2 cm in diameter), and it may be possible to cover the entire frequency range of 10 MHz to 3 GHz with a single probe. Further improvements in the temperature coefficient and in the response pattern of the probe are still needed, but are believed to be possible. The total uncertainty of this method would probably be less than about 0.5 dB. The biggest advantages of this approach are convenience, reliability, and simplicity.

CONCLUSION

Several methods of calibrating hazard meters have been discussed and the uncertainties associated with each method were estimated. It is important to understand that one cannot expect to achieve the same accuracy when using the meters for practical measurement applications. Some of the reasons are as follows.

1. Hazard meters are usually calibrated in nominally plane-wave fields. Such fields are seldom encountered in practice, and the sensor may not respond in the same way to non-planar fields.
2. In most calibration methods, only the sensor (probe) is exposed to the field, while in practice the complete system, including the indicating unit and connecting cable, is immersed in the field.
3. With hand-held meters, the presence of the operator can significantly affect the reading.

The additional uncertainty caused by these factors is difficult to assess and will vary with the type of meter. However, if good measurement procedures are followed, accuracies of $\pm$ 1 or 2 dB can probably be achieved in practice.

REFERENCES

1. ASLAN E.: *Narda Microwave Corporation* (private communication).
2. BOWMAN R.: *Proc. IEEE*, 1967, **55**, 981.
3. BOWMAN R. R.: *Some recent developments in the characterization and measurement of*

WHO – Biologic effects & health hazards of microwave radiation 1974

hazardous electromagnetic fields. Symp. on Biological Effects and Health Hazards of Microwave Radiation, Warsaw, 1973. Pol. Med. Publisher 1974.
4. BRAMALL K. E.: *J. Res. Natl. Bur. Std.* (U. S.), 1971, **75C**, 185, (July-December).
5. BRAUN E. H.: *Proc. of the I. R. E.*, 1953, **41**, 109 (January).
6. CHU T. S., SEMULAK R. A.: *Bell System Tech. J.*, 1965, **527** (March).
7. CRAWFORD M. L.: *Generation of standard EM fields using TEM transmission cells* (to be published).
8. ENGEN G. F.: *J. Res. Natl. Bur. Std.* (U. S.), 1971, **75C**, 89, (April-June).
9. HUDSON P. A.: *IEEE Trans. on Microwaves Theory and Techniques,* 1966, **MTT-14**, 293.
10. HUDSON P. A., SAULSBERY L. F.: *IEEE Trans. on Microwave Theory and Techniques,* 1971, **MTT-19**, 781.
11. JAKES W. C. Jr.: *Pro. IRE,* 1951, **39**, 161.
12. JULL E. V., DELOLI E. P.: *IEEE Trans. on Antennas and Propagation,* 1964, **AP-12**, 439.
13. JULL E. V.: *Electronics Letters,* 1970, **6**, 680.
14. KINBER B. Ye. TSEYTLIN V. B.: *Radio Engrg. and Electronic Phys.*, 1964, **9**, 1304.
15. NEWELL A. C., BAIRD R. C., WACKER P. F.: *IEEE Trans. on Antennas and Propagation,* 1973, **AP-21**, 418.
16. SCHELKUNOFF S. A.: *Electromagnetic Waves,* D. Van Nostrand, New York, 1943, p. 364.
17. SKAGGS G. A.: *High Frequency Exposure Chamber for Radiobiological Research,* NRL Memorandum Report 2218, 1971 (February).
18. SLAYTON W. T.: *Design and Calibration of Microwave Antenna Gain Standards,* NRL Report 4433, Naval Research Laboratory, Washington, D. C., November, 1954.
19. SOEJIMA T.: *Proc. I. E. E.*, 1963, **110**, 1021.
20. TSEYTLIN V. B., KINBER B. Ye.: *Radio Engrg. and Electronic Phys.* 1965, **10**, 10.
21. WOODS D.: *Non-ionizing Radiation,* 1969, **9** (June).

WHO – BIOLOGIC EFFECTS & HEALTH HAZARDS OF MICROWAVE RADIATION
1974

METHODS OF MICROWAVE FIELD QUANTIFICATION FOR BIOLOGIC STUDIES

R. B. Smith

Postgraduate School of Electrical and Electronic Engineering, University of Bradford, Bradford, United Kingdom.

In the United Kingdom, as in many countries, a continuous increase in the use of high-power microwave sources for radar, communication and heating applications, as well as the rapidly expanding literature on microwave radiation hazards, is resulting in a re-examination of the permissible radiation and emission levels and the means by which these levels are monitored. At the present time, there exists a United Kingdom national recommendation, which has been endorsed by the United Kingdom Medical Research Council, of a radiation level of 10 mW/cm² as a maximum limit for the continuous exposure of personnel. These levels are not intendend to be applied to therapeutic exposure under medical supervision.

Recently, in response to a number of requirements from sectors of United Kingdom industry and other official bodies, the Telecommunication Standards Committee of the British Standards Institute set up a technical committee to produce recommendations and prepare a British Standard on the "Safety of Telecommunication and Electronic Equipments, Components and Devices". This committee (TLE 23) consists of representatives from all the major United Kindgom telecommunication and electronic manufacturing industries, the Post Office, the Broadcasting Authorities, Government, Departments, National Research Organizations, technical branches of the Services, the Gas and Electricity Authorities, the Universities, oil companies and other organizations, together with such advisory bodies as the Medical Research Council, the United Kingdom Atomic Energy Authorities and various Government Department Safety Services.

The Committee is in the process of drafting a British Standard Guide, various parts of which are primarily intended for use by those concerned with the design, manufacture and usage of telecommunication and electronic equipment and the specifications and conditions of use of this equipment. It is intended that this guide will provide basic and fundamental information concerned with the hazards which may arise due to the design, operation and environmental conditions experienced with all types of telecommunication and electronic equipment. Standardized reproducible tests designed to assess the degree of safety in particular circumstances will be described, and recommended preferred methods of avoidance of possible hazards will be stated.

The Guide will be produced in a number of parts. The first part is intended to describe such general aspects as definitions and will include a method of classifying the seriousness of possible hazards of particular conditions of use for reference by manufacturers or users. All aspects, such as the stresses to which equipment might be subjected and the environmental conditions of use, the ability and training of personnel likely to have access to the equipment and the degree of such access, will be stated.

Subsequent parts of the Guide will describe the various hazards, their effects and suggested methods of protection, together with other related matters; attention will also be drawn where this is necessary to the anomalies and inconsistencies which may at present exist in other documents and indicate the preferred values and safety levels.

Subjects proposed for subsequent parts of the Guide are:

— Hazards associated with the use of electrical power in electronic equipment.
— Hazards associated with high and low temperatures.
— Mechanical, chemical and fire hazards associated with the use of electronic equipment.
— Radiation hazards.

Radiation hazards embrace:

— Ionizing radiation (X-rays, radioactive valves and substances and high voltages etc.).
— Hazards from light sources (ultraviolet light, infrared and lasers).
— Radio-frequency induced ignition and detonation.
— Non-ionizing radiation (the effects of non-ionizing radiation between 300 kHz and 30 GHz).

Priority has been given to the preparation and drafting of the part concerned with radiation. Working Parties have been established within the Committee to prepare draft recommendations on these sections. The Working Parties concerned with these activities are composed of experts and specialists in the particular field and are recruited from research organisations, universities, industry, and various Government Departments. A Draft for Development is being prepared by the Working Party responsible for the section on non-ionizing radiation hazards. The purpose of this Draft is to review the effects of electromagnetic radiation on the human body and to describe the work that has already been carried out, to determine the now acceptable power density which is considered safe for personnel engaged in, or working in the vicinity of, high-power radio frequency sources.

Radiation and emission standards and methods of monitoring power density are certainly important factors in maintaining a safe working environment. However the equipment manufacturer and the user are not expected to accept responsibility in setting radiation standards although they may possibly be expected to assume some degree of responsibility in monitoring power density and in ensuring that the standards are upheld.

In the United Kingdom the range of instruments produced by Narda are extensively used to measure power density. However, a programme of research on a novel type of radiation monitor was conducted in the United Kingdom by Fletcher and Woods (1) at the University of Surrey. Although this work did not result in a commercial instrument, it may be worthy of further consideration. The basic aim of the work was to produce an instrument which would measure the sum of the power densities due to any number of sources over a very wide frequency range. Measurement was to be independent of the direction of the incident power and of the angle of polarization. To this extent it would be similar to absorption by the human body.

The instrument is a bolometer based on the classical gas thermometer. Two thin-walled silica spheres are placed close together in a protective radome. The radome is coated to reflect infrared radiation, is transparent to microwave radiation and protects the spheres from unwanted draughts. The spheres are air-filled and connected by narrow diameter tube to a capacitive differential-pressure transducer. One sphere is coated with a resistive film and absorbs microwave energy. The other sphere is not coated and provides ambient temperature compensation. The pressure difference due to the absorption of energy by the resistive film and subsequent heating of the air in

WHO – BIOLOGIC EFFECTS & HEALTH HAZARDS OF MICROWAVE RADIATION 1974

the coated cylinder is converted into a change in capacitance at the pressure transducer, A special transformer ratio bridge converts the capacitance change into an out-of-balance voltage which is linearly related to temperature rise in the coated sphere and thus to the power absorbed.

The final temperature of the coated sphere is dependent on the heat loss mechanisms within the radome. The thermal time constant was found to be dependent mainly on the silica substrate and was about 8s for 63% of the final temperature. The use of an electronic differentiation circuit reduced the effective time constant of the instrument to less than one second.

A major part of the work was devoted to measuring the frequency-dependence absorption coefficient of the coated spheres. Absorption coefficient is defined as the ratio of the power absorbed by the sphere to the power incident on the area of cross-section of the sphere. Absorption coefficient was found to be a function of sphere diameter and surface resistivity. For the 3 cm diameter spheres chosen, the frequency response showed a damped resonance effect for coating resistivities below 5 kΩ/sq. The centre frequency occurred when the wavelength was approximately equal to one quarter of the sphere diameter. The maximum absorption coefficient of 1.77 was for a coating resistivity of 200 Ω/sq, about half the wave impedance. These results were confirmed theoretically by Williams (2). A coating resistivity of 5 kΩ/sq gave a reasonably uniform response from 400 kHz to 5.5 GHz. Additional spots or platelets of surface resistivity 200 Ω/sq painted on the surface of the resistive film extend the frequency response to 35 GHz.

REFERENCES

1. FLETCHER K. A., WOODS D.: *Non-ionizing Radiation,* 1969, 1, 57 (September).
2. WILLIAMS W. E.: *Proc. IEEE,* 1970, 117, 2236 (December).

WHO – Biologic effects & health hazards of microwave radiation
1974

RADIATION HAZARDS FROM MICROWAVE SOURCES WITH MOBILE ANTENNAS: CERTAIN TECHNICAL PROBLEMS

Z. Frank

Institute of Aviation Medicine, Prague, Czechoslovakia

The problems of the interaction between microwave radiation and man may be considered from many points of view; detailed references may be found in recent publications by Gordon (3) and Marha (4). It may by assumed that the possibility of deleterious health effects is sufficiently well documented. In considering hygienic problems legal safe exposure limits should be taken as a starting point. Particular attention in considering hygienic conditions in a given locality should be paid to microwave sources, the main function of which is to emit energy into the environment. Typical sources of this kind are radar installations.

The objectivity of the evaluation of hygienic conditions depends on certain basic conditions, i.e. the choice of the measured physical parameter of the radiation, the choice of the measuring equipment and methods, as well as the methods of evaluation of results. These basic conditions will be not discussed here and are taken for granted. Mumford's paper (5) may be considered as the best source of data concerning technical aspects of hygienic evaluation of microwave hazards. These aspects are inherently related to the theory of antennas and microwave propagation. In the present state of the art the general practice is to measure the intensity of the irradiated field, the basic conditions being a certain minimal distance between the sensor and the emitting antenna.

It should be pointed out that real conditions during field measurements of microwave intensity differ great from those of calibrating stands and in anechoic chambers To evaluate the permissibility of the conditions for human exposure it is necessary to determine the maximal intensity values. These change in time according to the regime of work of radar equipment, the changes being in most cases aperiodic. Moreover the radiation emitted from several independent sources simultaneously should be taken into account. The question arises of how to approach the problem of valid evaluation of the hygienic conditions in the case of sources with mobile antennas. The principal consideration is of course the health safety of the exposed individual. It should be, remembered, however, that overestimation of the hazards may have serious economic consequences. The aim of this paper is to present certain approaches to the problem of evaluation of the hygienic conditions.

Measurement of fields irradiated by various radar types are made using thermistor sensors and the measured parameter is the power density. If the measurements are made at various distances with the antenna immobile, varying the distance and position in respect to the axis of the beam, a certain spatial horizontal characteristic of the power density is obtained. If these results are analyzed and idealized (i.e. reflections are neglected) a characteristic power density distribution may be obtained for a given type of radar. This does not allow of course for movement of the antenna and the "inter-

mittent" type of exposure, which is illogical. Such procedure is used, however, to define safe and hazardous zones.

This procedure is inconvenient because it is time consuming and needs complex calculations. It should also be stressed that the real hygienic conditions are different from such bidimensional characteristics and change with a change in the direction of the radiated beam. This procedure cannot be used in the case of a projected new localization for a radar installation. In such a case an approximate calculation may be made and the permissibility of such a proposed localization evaluated. Theoretically it is possible to predict the field intensity at an arbitrary point given the characteristics of the antenna, the power of the source and characteristics of the terrain along the direction of the beam. These theoretical predictions differ in many instances from the results of practical measurements in real conditions.

It may be difficult to determine the power density distribution in the case of certain directional antennas on the basis of diagrams of radiation characteristics. In theory there exist numerous formulas for the determination of antenna characteristics. In practice, however, it is necessary to verify theoretical calculations by practical measurements. Several of the variables important from the point of view of hygienic-technical considerations are unknown. The problem may be reduced to the question of adequate formulas for the determination of directional characteristics of the antennas on the basis of their design and dimensions. Such formulas are valuable for hygienic-technical services.

The problem of the determination of radiation distribution diagrams of antennas may be evaluated less pessimistically if functions of the type:

$$\frac{\sin\alpha}{\alpha},\ \cos^2\alpha,\ e^{-\alpha^2},\ \frac{\cos\alpha}{1-(\frac{2}{\pi}\alpha)^2},\ \frac{2J_1(\alpha)}{\alpha} \qquad [1]$$

(J_1 = Bessel function of the first order) are used. Comparing such solutions with real radiation distribution diagrams it may be said that such functions may be used for hygienic evaluation, if the width of the beam is considered to be one half of the maximal power density value. Data on the width of the beam may be found in technical documentation on radar, but such documentation must be evaluated critically. It should be stressed that uniform distribution of power density along axes of the beam is a theoretical case, rarely corresponding to the real distribution. Difficulties may be encountered particularly in the case of narrow beams.

Particular attention should be paid to the elevation of antennas which are vertically mobile. The angle of elevation influences not only the power density at a given point but also the width of the beam.

In may be said that in the case of mobile antennas it may be more convenient to evaluate hygienic conditions not on the basis of power density measured or calculated, but on the basis of the sum of energy radiated during a given time (e.g. during one day). This would correspond to the approach (6) of considering the reactions of the human organism to microwaves on the basis of a time-weighted average dose.

For hygienic evaluation purposes the reflection from earth cannot be neglected in many instances. This may be calculated if one considers a fictitious radar representing the secondary source acting as a mirror with respect to the primary source. Adequate corrections for the measured power density should be introduced taking the polarization, reflection angles, etc. into account.

The evaluation of reflections is difficult and in certain instances (2) may make the whole hygienic evaluation doubtful. Parasitic frequencies and their influence on the microwave dose should be also taken into account.

WHO – BIOLOGIC EFFECTS & HEALTH HAZARDS OF MICROWAVE RADIATION 1974

In real conditions a given point is usually irradiated from several sources simultaneously and the resulting arithmetical sum of power densities should be accepted for hygienic evaluation.

Taking all the above points into consideration, an orderly sequence of theoretical analysis, real measurements, analysis of the real existing situation and of all the factors influencing the distribution of power density from the antennas of the equipment used, may serve for elaboration of formulas for computation of data for hygienic evaluation of working conditions. Such formulas adapted to the characteristics of the radar considered in each particular instance may serve also for prediction of the hygienic conditions in the case of new installations.

REFERENCES

1. DRABKIN, A., L., ZUZENKO, V., L.: *Antěnno-fidernye ustroystva.* Sovetskoe radio, Moskva, 1961.
2. GLASER, Z., R., HEIMER, O., M.: Determination and Elimination of Hazardous Microwave Fields Aboard Naval Ships. In: *IEEE Transactions on Microwave Theory and Techniques,* February 1971, **MTT-19**, 2, 232.
3. GORDON, Z., V.: *Voprosy gigieny truda i biologičeskogo deistvija elektromagnitnyh polei sverkhvysokikh častot.* Medicina, Leningrad, 1966.
4. MARHA, K., MUSIL, J., TUHÁ, H.: *Elektromagnetické pole a životni prostředi.* Státni zdravotnické nakladatelství, Praha, 1968.
5. MUMFORD, W., W.: Some Technical Aspects of Microwave Radiation Hazards. In: *Proceedings of I. R. E., Vd. 49,* February 1961, p. 427.
6. SAVIN, B., M., SUBBOTA, A., G., ČUHLOVIN, B., A., SYNGAJEVSKAJA, V., A., ŽURAVLEV, V., A., SVETLOVA, Z., P.: O količestvennoj zavisimosti bioeffektov SWČ polja ot PPM i ekspozicii. In: *Gigiena truda i biologičeskoe dejstvie elektromagnitnyh voln radiočastot,* Institut gigieny truda i proffessionalnykh zabolevani AMN USSR. Moskva, 1972, p. 90.

WHO – BIOLOGIC EFFECTS & HEALTH HAZARDS OF MICROWAVE RADIATION 1974

RESONANCE METHOD FOR THE DETERMINATION OF THE COMPLEX DIELECTRIC CONSTANT OF BIOLOGIC MATERIALS IN THE MICROWAVE BAND

M. Piotrowski

Military Institute of Hygiene and Epidemiology, Warsaw, Poland

Knowledge of the electric parameters of tissues is highly useful and makes it possible, among other things, to draw conclusions about propagation conditions and energy absorbed by objects placed in the electromagnetic field. From the metrological point of view, the problem resolves itself into the determination of the complex dielectric constant $\varepsilon = \varepsilon' - j\varepsilon''$ of biologic materials with a large real component ε' and an imaginary component ε'', with magnetic inductive capacity equal to the permeability of vacuum $\mu_o = 1$.

The problem of measuring the complex dielectric constant has been solved using the resonance method, assuming that the examined substance was placed in a cuvette, the dimensions of which were smaller than the inner dimensions of the measuring cavity. Losses in the walls of the cuvette and its geometry were taken into consideration.

Difficulties typical for resonance methods and connected with materials which have high dielectric constants and at the same time great losses can be partly avoided by placing samples in a weak electric field. Such measuring conditions are guaranteed by cylindrical resonators with field distribution of quasi-H_{O11}* made where the examined substance is placed concentrically (Fig. 1).

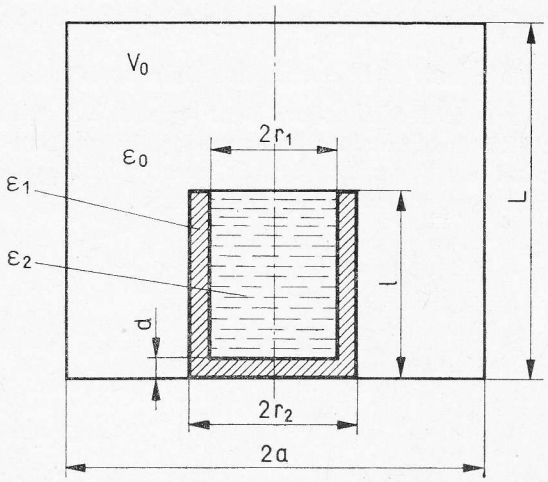

Fig. 1. Measuring cavity.

* The definition of quasi-H_{011} is understood as a kind of free vibration of the resonator which changes into the H_{011} mode when the disturbance is removed.

WHO – BIOLOGIC EFFECTS & HEALTH HAZARDS OF MICROWAVE RADIATION 1974

Such a system makes it possible to obtain a high Q factor, easy re-tuning by contactless short-circuiting switch and large attennuation of undersirable modes. Simple technology ensures tolerances in building the cavity and in preparing samples in cuvettes for examined liquids.

There are two aspects to the realization of this task:

First — the electrodynamic aspect which may be reduced to the solution of the internal electrodynamic problem for the case of an isotropic medium described in compartments by a continuous function of dielectric permittivity of a nonhermitian symmetry (which means the occurrence of losses) filling the cavity incompletely;

Second — the metrologic aspect based on experimental determination of the resonance frequency and the Q factor of the resonator with and without a sample, and establishing interrelations linking these quantities with certain physical parameters of the resonator and the examined material.

Geometric heterogeneity and existence of losses in the examined material are the reason for difficulties in arriving at an analytical description of electromagnetic effects. The accurate solution of such a problem is not known.

So far, attempts to solve these problems by a perturbation method, as one of a number of similar general methods of analysis, have been made.

The condition of low disturbance*, which is connected with this method, has narrow limits both electric and geometric, and limits the range of application and the precision of the results obtained.

Lack of formal criteria of error evaluation makes it necessary to evaluate deviations by an indirect way estimating by approximation of disturbed fields or by experimental verification.

The problem can be solved with arbitrary accuracy by projection methods, based on an initial approximate equation and then an accurate solution of the approximate equation. Generally, approximate equations are composed in such a way that problems described by differential or integral linear operators are resolved into solving of a finite set of algebraic equations. Galerkin's method is one of the general projection methods of analysis. This method belongs to a group of methods, in which the solutions are looked for in a form of expansion into series of functions according to a complete set of functions.

In practice, Galerkin's method has been applied direct to Maxwell's equations (14). The sought field vectors $\vec{E}$, $\vec{H}$ and inductions $\vec{B}$, $\vec{D}$ were developed into series [1.1] in a complete set of self-functions obtained from solving the problem of an empty resonance cavity which has ideally conductive walls, exactly the same dimensions as the measuring resonator, and from the created electrodynamic basis.

$$\begin{aligned}
\vec{B}^N &= \mu_0 \sum_{n=1}^{N} b_n \vec{H}_n ; \\
\vec{D}^N &= \varepsilon_0 \sum_{n=1}^{N} a_n \vec{E}_n ; \\
\vec{E}^N &= \sum_{n=1}^{N} c_n \vec{E}_n + \sum_{n'=1}^{N'} c_{n'} \vec{E}_{n'} ; \\
\vec{H}^N &= \sum_{n=1}^{N} d_n \vec{H}_n + \sum_{n'=1}^{N'} d_{n'} \vec{H}_{n'}
\end{aligned} \qquad [1.1]$$

---

* Even though Rayleigh-Schroedinger's method of disturbance calculations is not subordinated to low disturbance criteria, its utility in electrodynamics is insignificant.

Formulas for the first approximation of the theory are generally speaking less accurate than quasi-statistical approximations of the conventional theory of disturbance, and complex algorithms (sets of differential equations) are difficult to use.

Expansion factors a, b, c and d are determined by solving the matrix set of equations expressed by following algorithms:

$$(\Omega \overset{\wedge}{\ni} \Omega \hat{M})^{-1} \underline{b} = \frac{1}{(\omega_N)^2} \underline{b}; \qquad \text{[I]}$$

$$(\Omega \hat{M} \Omega \overset{\wedge}{\ni})^{-1} \underline{a} = \frac{1}{(\omega_N)^2} \underline{a}; \qquad \text{[II]}$$

$$\Omega^{-1} \left\{ \overset{\vee}{M} - \overset{\vee}{M} (\overset{\vee}{M})^{-1} \overset{\vee}{M} \right\} \Omega^{-1} \left\{ \overset{\vee}{\ni} - \overset{\vee}{\ni} (\overset{\vee}{\ni})^{-1} \overset{\vee}{\ni} \right\} C = \frac{1}{(\omega_N)^2} C \qquad \text{[III]}$$

$$\overset{\vee}{M} \Omega^{-1} \ni \Omega^{-1} b = \frac{1}{(\omega_N)^2} b; \qquad \text{[IV]}$$

where:

Ω = diagonal matrix created from resonant pulsation of an empty cavity;

M = matrix describing magnetic characteristics of medium which is inside the cavity;

$\ni$ = matrix describing electric characteristics of medium and similar to matrix M made of elements in a form of scalar products;

$$\overset{\wedge}{\ni}_{kn} = \varepsilon_0^2 \left(\overset{\leftrightarrow}{\varepsilon}^{-1} \vec{E}_n, \vec{E}_k \right), \quad \overset{\vee}{\ni}_{kn} = \left(\overset{\leftrightarrow}{\varepsilon} \vec{E}_n, \vec{E}_k \right), \qquad \text{[1.2]}$$

$$\hat{M}_{kn} = \mu_0^2 \left(\overset{\leftrightarrow}{\mu}^{-1} \vec{H}_n, \vec{H}_k \right), \quad \overset{\vee}{M}_{kn} = \left(\overset{\leftrightarrow}{\mu} \vec{H}_n, \vec{H}_k \right).$$

In the given model of cylindrical cavity with concentrically placed sample of lossy dielectric, which is the scalar centre, given algorithms have simpler forms. In that case, matrix of M type is elementary (unitary). This is a result of the "magnetic" homogeneity of the medium placed inside the resonator ($\mu = 1$) and the arbitrary normalization. As a result of the symmetry peculiar to quasi-H_{onp} modes, only tangential components of the electric field exist in the examined sample. This means that conditions allowing the development of the electric field $\vec{E}$ in the electric sub-set of sourceless functions ($C_n = O$) hawe been fulfilled, i. e., div $\vec{E} = O$ and the normal component is continuous on the arbitrary surface inside V (with $E \in D_{div}$).

As a result, in the algorithm III used later on, besides the diagonal matrix Ω^{-1}, and the elementary matrix $\overset{\vee}{M}$, only matrix $\overset{\vee}{\ni}$ is left. Also for the algorithm II, the complete basis consists of a set of rotational functions. Vector $\vec{a}$ corresponds to the expansion of induction $\vec{D}$ which for closed surfaces without source (charge) always develops in the set of sourceless functions.

After complex conversions, formulae for certain elements of matrix A describing the analysed internal problem, are obtained [1.3].

$$A c_i = \Lambda_i c_i \qquad \text{[1.3]}$$

$$\Lambda_i = \Lambda + j\Lambda'' = \frac{1}{a^2 \varepsilon_0 \mu_0 \omega_N^2}$$

In the formulae in Table 1 the indexes m, n, p mean:

m — order of Bessel's functions,

n — next element of Bessel's function,

p — visualizes field distribution along the resonator axis.

Structure of the programmed matrix is shown in Figure 2.

Eigen-value Λ i and eigen-vectors Ci of complex matrices A were calculated according to

WHO – Biologic effects & health hazards of microwave radiation 1974

TABLE 1
Formule

1. Diagonal words for $m = m' = 0$, $n = n'$ and $p = p'$

$$A_{ii} = \left[\mu_{on}^2 + \left(\frac{p\pi a}{L}\right)^2\right]\left\{1 + \frac{1}{J_0^2(\mu_{on})}\left[\left(\frac{1}{\varepsilon_1} - 1\right)\left(\frac{l}{L} - \frac{\sin 2\pi p \frac{l}{L}}{2\pi p}\right) I'\left(\mu_{on}\frac{r_2}{a}\right) + \right.\right.$$
$$\left.\left. + \left(\frac{1}{\varepsilon_2} - \frac{1}{\varepsilon_1}\right)\left(\frac{l}{L} - \frac{\sin 2\pi p \frac{l}{L}}{2\pi p} - \frac{d}{L} + \frac{\sin 2\pi p \frac{d}{L}}{2\pi p}\right) I'\left(\mu_{on}\frac{r_1}{a}\right)\right]\right\}$$

2. Non-diagonal words for $m = m' = 0$, $n \neq n'$ and $p = p'$

$$A_{ij} = \frac{2\left[\mu_{on}^2 + \left(\frac{p\pi a}{L}\right)^2\right]}{(\mu_{on}^2 - \mu_{on'}^2)\cdot J_0(\mu_{on})\cdot J_0(\mu_{on'})}\left[\left(\frac{1}{\varepsilon_1} - 1\right)\left(\frac{l}{L} - \frac{\sin 2\pi p \frac{l}{L}}{2\pi p}\right) I_1'\left(\mu_{on}\mu_{on'}\frac{r_2}{a}\right) + \right.$$
$$\left. + \left(\frac{1}{\varepsilon_2} - \frac{1}{\varepsilon_1}\right)\left(\frac{l}{L} - \frac{\sin 2\pi p \frac{l}{L}}{2\pi p} - \frac{d}{L} + \frac{\sin 2\pi p \frac{d}{L}}{2\pi p}\right) I_1'\left(\mu_{on}\mu_{on'}\frac{r_1}{a}\right)\right]$$

3. Non diagonal words for $m = m' = 0$, $n = n'$ and $p \neq p'$

$$A_{ij} = \frac{\mu_{on}^2 + \frac{p\pi a}{L}}{\pi J_0^2(\mu_{on})}\left\{\left(\frac{1}{\varepsilon_1} - 1\right)\left(\frac{\sin\pi(p-p')\frac{l}{L}}{p-p'} - \frac{\sin\pi(p+p')\frac{l}{L}}{p+p'}\right) I'\left(\mu_{on}\frac{r_2}{a}\right) + \right.$$
$$\left. + \left(\frac{1}{\varepsilon_2} - \frac{1}{\varepsilon_1}\right)\left[\frac{\sin\pi(p-p')\frac{d}{L}}{p-p'} - \frac{\sin\pi(p+p')\frac{l}{L}}{p+p'} - \frac{\sin\pi(p-p')\frac{d}{L}}{p-p'} + \frac{\sin\pi(p+p')\frac{d}{L}}{p+p'}\right] I'\left(\mu_{on}\frac{r_1}{a}\right)\right\}$$

4. Non-diagonal words for $m = m' = 0$, $n \neq n'$, $p \neq p'$

$$A_{ij} = \frac{2\left[\mu_{on}^2 + \left(\frac{p\pi a}{L}\right)^2\right]}{\pi(\mu_{on}^2 - \mu_{on'}^2)\, J_0(\mu_{on})\, J_0(\mu_{on'})}\left\{\left(\frac{1}{\varepsilon_1} - 1\right)\left(\frac{\sin\pi(p-p')\frac{l}{L}}{p-p'} - \frac{\sin\pi(p+p')\frac{l}{L}}{p+p'}\right) I_1'\left(\mu_{on}\mu_{on'}\frac{r_2}{a}\right) + \right.$$
$$\left. + \left(\frac{1}{\varepsilon_2} - \frac{1}{\varepsilon_1}\right)\left(\frac{\sin\pi(p-p')\frac{l}{L}}{p-p'} - \frac{\sin\pi(p+p')\frac{l}{L}}{p+p'} - \frac{\sin\pi(p-p')\frac{d}{L}}{p-p'} + \frac{\sin\pi(p+p')\frac{d}{L}}{p+p'}\right) I_1'\left(\mu_{on}\mu_{on'}\frac{r_1}{a}\right)\right\}$$

where

$$I'\left(\mu_{on}\frac{r_{1,2}}{a}\right) = \left(\frac{r_{1,2}}{a}\right)^2\left[J_0^2\left(\mu_{on}\frac{r_{1,2}}{a}\right) + J_1^2\left(\mu_{on}\frac{r_{1,2}}{a}\right) - 2\frac{J_1\left(\mu_{on}\frac{r_{1,2}}{a}\right) J_0\left(\mu_{on}\frac{r_{1,2}}{a}\right)}{\mu_{on}\frac{r_{1,2}}{a}}\right]$$

$$I_1'\left(\mu_{on}\mu_{on'}\frac{r_{1,2}}{a}\right) = \left(\mu_{on'}\frac{r_{1,2}}{a}\right) J_1\left(\mu_{on}\frac{r_{1,2}}{a}\right) J_0\left(\mu_{on'}\frac{r_{1,2}}{a}\right) - \left(\mu_{on}\frac{r_{1,2}}{a}\right) J_1\left(\mu_{on'}\frac{r_{1,2}}{a}\right) J_0\left(\mu_{on}\frac{r_{1,2}}{a}\right)$$

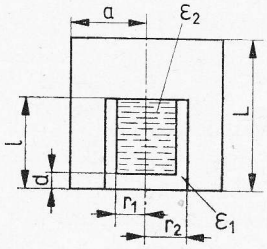

WHO – BIOLOGIC EFFECTS & HEALTH HAZARDS OF MICROWAVE RADIATION
1974

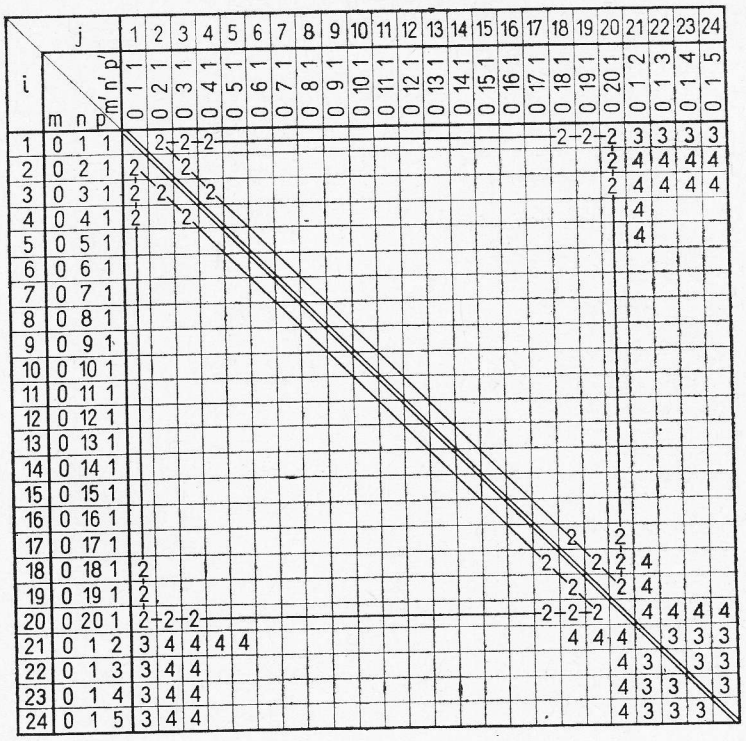

Fig. 2. Structure of matrix A.

Wielandt's method (10). The set of equations for N = 20 was solved on an Odra 1204 computer. The derived formulae are not limited and can be used for any N (size of basis). We have calculated:

1. The geometric characteristics (Fig. 3 and 4).

These show, that if the diameter of the sample increases the changes in f and Qd are bigger in comparison with the changes caused by the same gains in the height of the sample.

2. The electric characteristics f (ε'_2, ε''_2) (Fig. 5 and 6) from which, knowing from measurements the Q factor Qd, it is easy to determine ε'_2 and knowing the frequency of the resonator we can determine ε''_2 of the examined material.

EXPERIMENTAL TESTING OF DIELECTRIC PARAMETERS

The basic element of the measuring (testing) set is a resonator (Fig. 7) tunable to the X band with a field distribution H_{O11}. Two holes, symmetrically placed at the bottom of the cavity couple the resonator with the activating generator.

Coupling of the resonator with the detection set is ensured by a hole in the side of the cylinder at an angle of 45° to the axis going through the activating holes. On the inside walls of resonator, a gold layer of 10 μm has been deposed by electroplating. Measuring sets for determining the Q factor and resonator frequency are shown on Figure 8 and 9.

WHO – Biologic effects & health hazards of microwave radiation 1974

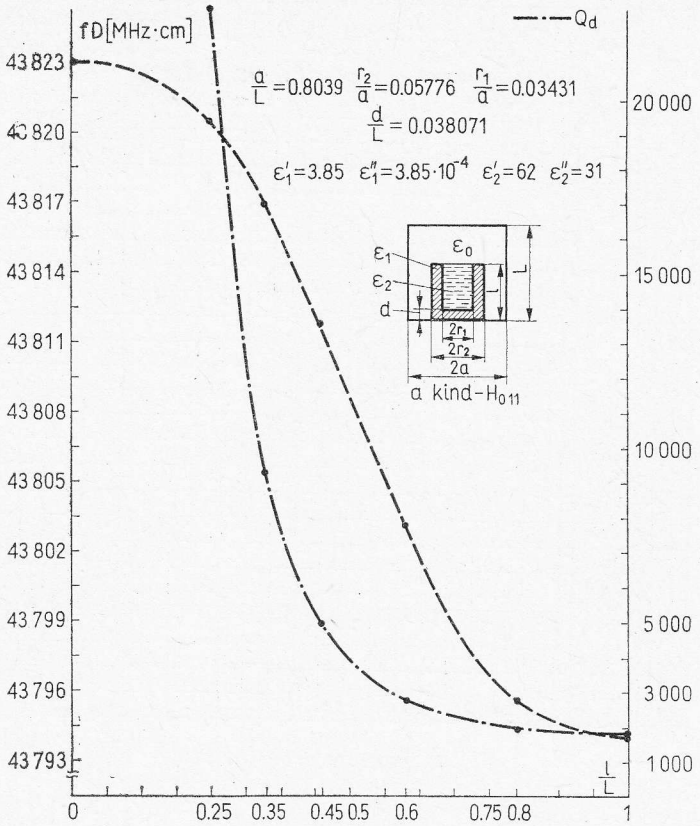

Fig. 3. Resonant frequency of H_{011} mode and Q factor conditioned only by losses in the sample as a function of the height of the sample.

Resonant frequency in band X was measured by a wavemeter Cz-3-44 (Fig. 8). Besides determining the maximum of the resonant curve by simple measurement (ensuring fine tuning accuracy $\frac{\Delta f}{f} \geqq \frac{1}{10\,Q}$) a method based on the symmetry of the resonant curve has been used, for which the fine tuning indicator eliminates the distortions (peaks) existing on peaks of the pulse output signal.

The transmission set for measuring the Q factor (Fig. 9) ensures visualization of the resonant curve on one trace of the dual trace oscilloscope and measurement of the width of the resonant curve by the use of calibration markers on the second trace.

The second trace is also, when necessary, used for controlling the generation zone of a reflex klystron with modulated frequency (GK-4-19A). Half-power level on the resonator curve was determined by introducing a 3 db attenuation through a master attenuator, X-113, into the transmission line.

Using this method, measurements of the dielectric constants of a number of biologic substances have been carried out (16). An example of the results of these measurements is shown in Table 2, together with the corresponding biologic material.

WHO – Biologic effects & health hazards of microwave radiation 1974

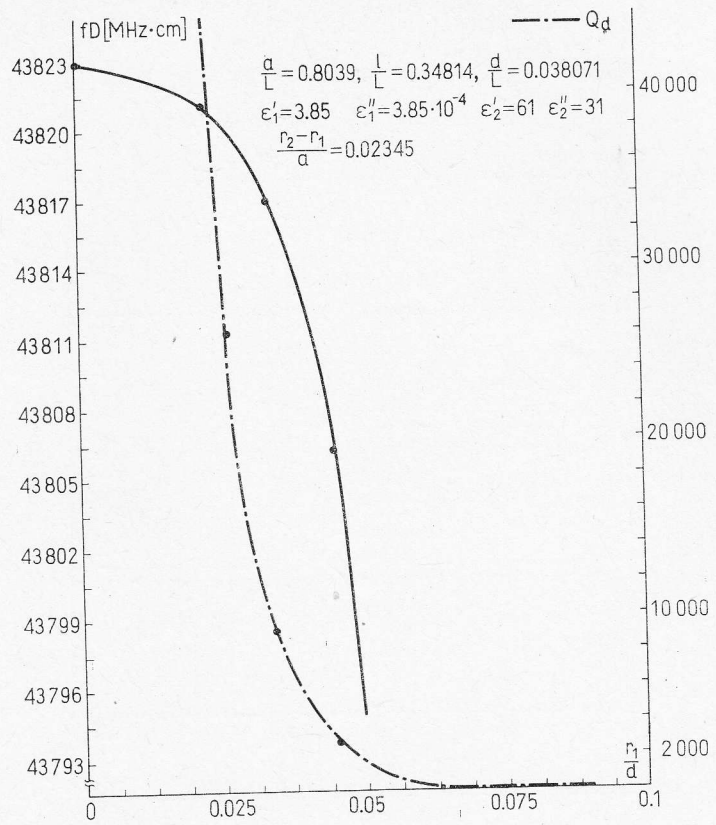

Fig. 4. The same quantities (as Fig. 3) but as a function of the diameter of the sample.

Table 2

Result

Material	Q factor of resonator with cuvette		Tuning with empty cuvette	Dielectric constant	
	Q_D	Q	Δf [kHz]	ε'_2	ε''_2
Distilled water	9650	4420	1010	61	33.5
Gamma-globulin	9650	4050	1100	66	38.0
Human blood (Na tartrate)	9650	4870	780	47	27.5

A comparison of our results with the information avilable in the literature shows agreement within the accuracy of the methods of measurement.

WHO – BIOLOGIC EFFECTS & HEALTH HAZARDS OF MICROWAVE RADIATION
1974

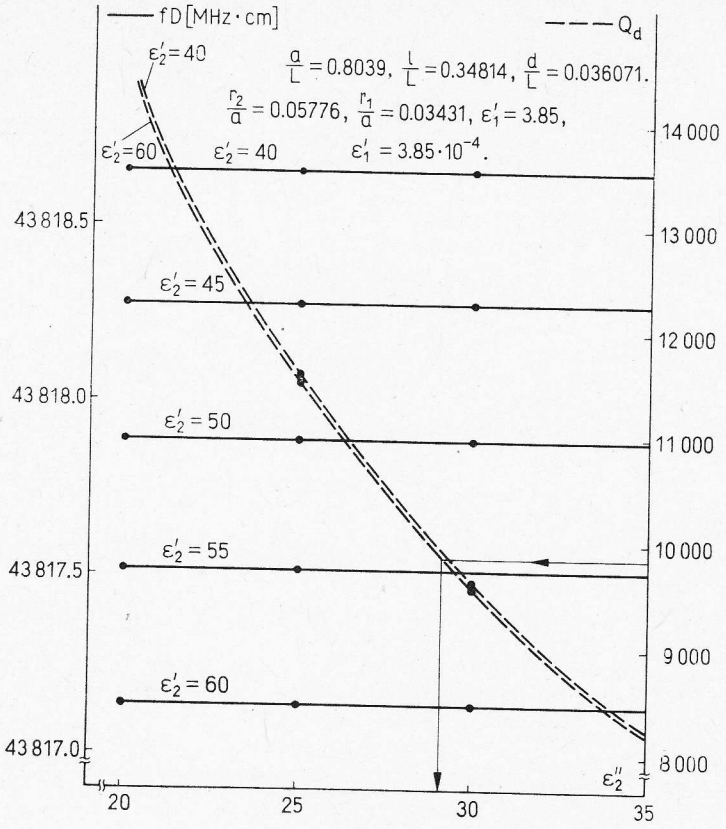

Fig. 5. Electrical characteristics.

CONCLUSIONS

Recapitulating, it is worth noting that the accurate solution of the problem is not known. Using Galerkin's method, an original solution of the problem of self vibrations of the measuring resonator has been obtained.

An analytical procedure and the use of quasi H_{onp} modes are needed for the dielectric measurement of lossy samples concentrically placed in the resonator and cuvettes, not fully filling the cavity (increasing the size of the sample to fill the cavity is a special case of the obtained dependence). There are no restrictions on size or on the material parameters of the tested substances (for isotropic media with magnetic permeability equal to vacuum permeability $\mu_o = 1$).

The characteristics mentioned here allow the choice of samples convenient for the experiment and ensure obtaining the selected sensitivity for predicted values of ε_2 and ε_1. It is evident that the most critical parameter is the inside diameter of the cuvette, for which the necessary accuracy of measurement is:

$$\frac{\Delta r_1}{r_1} \leqq 1{,}5 \cdot 10{-}2$$

WHO – BIOLOGIC EFFECTS & HEALTH HAZARDS OF MICROWAVE RADIATION 1974

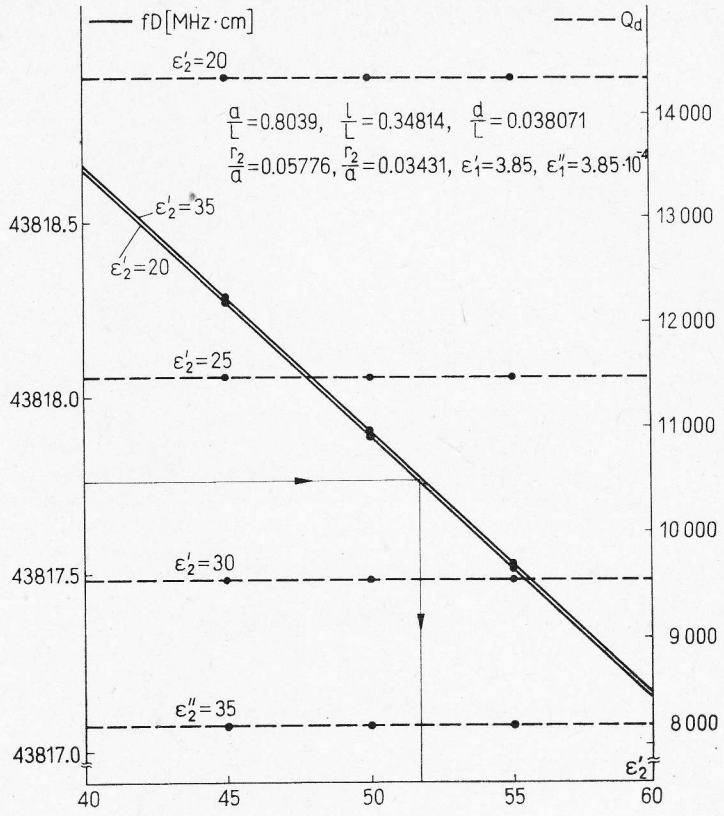

Fig. 6. Electric characteristics.

The introduction of reduced dimensions, related to the diameter of the cavity, facilitates the use of diagrams and formulae to select a range of frequencies for with the use of the resonance method is practical.

The procedure for determining the permittivity ε'_2 and ε''_2 from f (ε', ε'') and Qd (ε', ε'') may be carried out separately.

In the range of measured values $\varepsilon'_2 = (40 + 60)$ and $\varepsilon''_2 = (20 + 35)$ the error made does not exceed 0.5%. The full error in determining ε'_2 and ε''_2 is mainly due to the measuring technique used, and is (5 + 10)%.

The program worked out (16) makes it possible to introduce changes for various conditions of measuring the complex dielectric constant quickly.

* * *

Much valuable advice and many critical comments helped me to prepare this paper. I would like to thank very much all concerned and specially Prof. Dr. Ludwik Badian, Dr. Mirosław Dąbrowski and Eng. Andrzej Szubski.

WHO – BIOLOGIC EFFECTS & HEALTH HAZARDS OF MICROWAVE RADIATION 1974

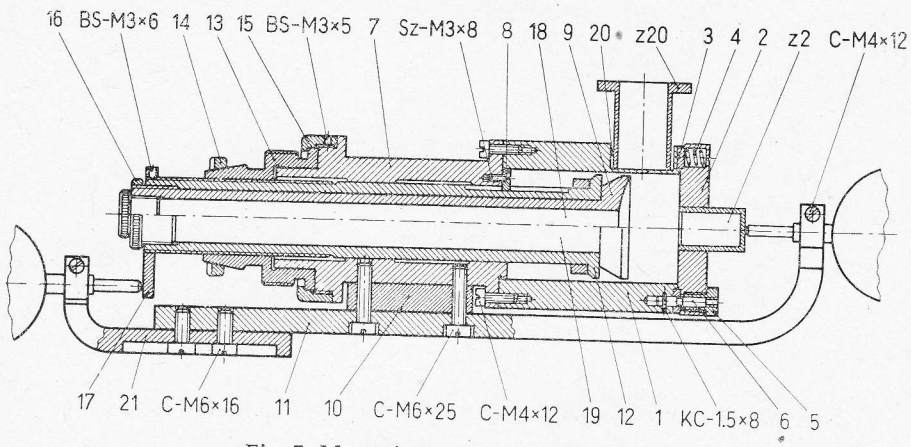

Fig. 7. Measuring resonator for X-band.

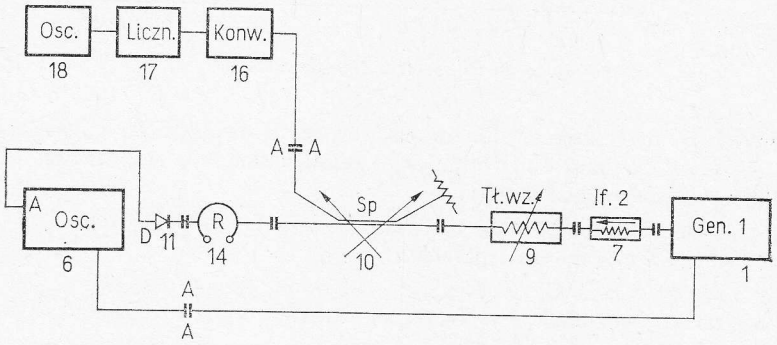

Fig. 8. Block diagram of the set for measuring resonance frequency. Symbols: Gen. 1 — type GK4-19A sawtooth wobbled generator, 3 cm band, Osc. — type OKD-505A dual trace oscilloscope with time base output, If 1 — type X101A ferrite insulator, If 2 — type X103 ferrite insulator, Tł. wz. — type X130 standard attenuator. Sp. — type X121 10 dB directional coupler, D — detector, *Konw.* — type Cz4-7 frequency converter, Liczn. — type Cz3-4A frequency digital counter.

WHO – Biologic effects & health hazards of microwave radiation 1974

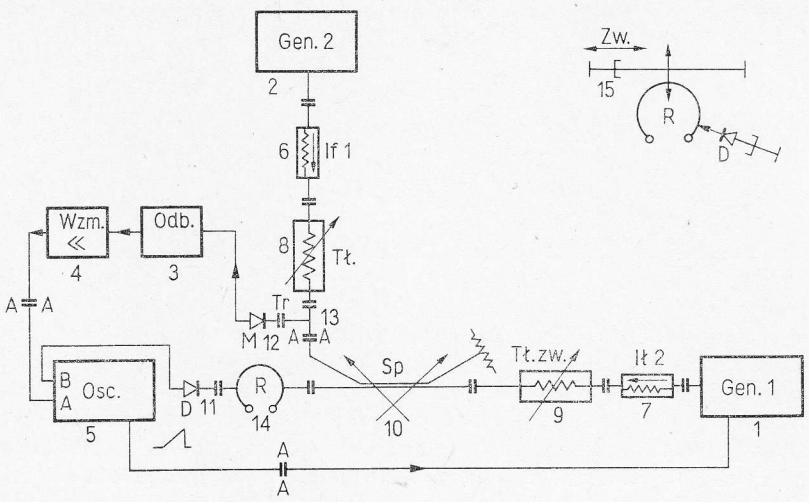

Fig. 9. Block diagram of the set for the measuring resonator band. Symbols: Gen. 1 — type GK4-19A sawtooth wobbled generator, 3 cm band, Gen. 2 — type G3-14A non-modulated generator, 3 cm band, Odb. — Type Lambda receiver, Wzm. — acoustic amplifier (own manufacture), Osc. — type OKD-505A dual trace oscilloscope with time base output, If 1 — type X101A ferrit insulator, If 2 — type X103 ferrit insulator, Tł. — type X134 non-calibrated attenuator, Tł. wz. — type X130 standard attenuator, Sp. — type X121 10 dB directional coupler, D — detector, M — mixing head, Tr. — type X153 T joint, R — the investigated resonator, Zw. — type X112 regulated contact.

REFERENCES

1. BADIAN L.: *Prace PIT*, 1965, **47/48**, 15.
2. BOCHENEK K.: *Metody analizy pól elektromagnetycznych*, PWN, Warszawa—Wrocław, 1961 (Pol.).
3. BRANDT A. A.: *Issledovanija dielektrikov na swierhwysokih častotah*, Moskva 1963.
4. CASIMIR H. B. G.: *Philips Rew. Repts.*, 1951, **6**, 1, 162.
5. COOK H. F.: *Brit. J. of Applied Physics*, 1952, 3, 8, 249.
6. GRANT E. H.: *Ann. N. Y. Acad. Sci.* 1965, **125**, 418.
7. GINZTON E. L.: *Miernictwo mikrofalowe*, PWT, Warszawa 1961 (Pol.).
8. GRIFONE L.: *Alfa Frequenza*, 1957, 26, 580.
9. HARVEY A. F.: *Microwave engineering*, Academic Press, London 1963.
10. HAUSSHOLDER A. S.: *The theory of matrices in numerical analysis*, Blaisdell Publishing Company 1964.
11. KRASNOSELSKI M. A. et al.: *Približennoe rešenie operatornyh uravnieni*, Moskva, 1969.
12. MICHLIN S. G.: *Varjacionnye metody w matematičeskoi fizykie*, Moskva, 1957.
13. NIKOLSKY W. W.: *Varjacionnye metody dla vnutriennyh zadač elektrodynamiki*, Moskva, 1967.
14. NIKOLSKY W.: *Radiotehnika i Elektronika*, 1957, **2**, 7

MICROWAVE REFLECTION AND DIFFRACTION BY MAN

D. E. Beischer and V. R. Reno

Naval Aerospace Medical Research Laboratory, Pensacola, Florida, U. S. A.

A study of the biologic effects of low-intensity microwave energy on man is in progress at our laboratory. To appraise the subtle effects of microwave radiation below an intensity of 10 mW/cm² an understanding of the fundamentals of microwave dosimetry and the use of new and improved measurement methods seemed necessary. The present investigation is specifically concerned with a study of the spatial energy distribution in proximity to man as a function of the radiation parameters. It is evident that only the field inside the body of man is relevant for judging biological radiation effects, but it is expected that valuable information contributing to the evaluation of these fields will be gained from measurements of the reflected, scattered and transmitted radiation around man. Measurements of the spatial energy distribution in proximity to man automatically take into account the complex shape and size of man and his electromagnetic as well as dynamic structure. Our approach will be to relate such measurements to similar measurements and calculations on simpler objects where the physical principles of reflection, diffraction and transmission are well understood. Since such calculations and measurements are based mostly on plane wave incident radiation, we have tried to approach this condition experimentally.

Our facility uses a large parabolic reflector (4.8 m diameter) to collimate the beam which illuminates an experimental stage (3.6 m by 3 m by 2.4 m). Any frequency between 1 and 12.4 GHz can be obtained in either continuous wave, pulsed or swept mode and in vertical or horizontal polarization. Either AM or FM modulation is available. Monochromatic radiation is assured by filtering during single-frequency operation, and multi-frequency operation is possible.

Power measurements are based on recent concepts and instrumentation developed and provided by the National Bureau of Standards (2). The high sensitivity and small size of this isotropic sensor permit very low power levels (in the μW/cm² range) to be measured with a high degree of spatial resolution. The energy distribution throughout the experimental space is measured by automatic scanning of a series of vertical or horizontal planes. The effects of selected objects on the pattern of the energy distribution are readily visualized by comparison of the unperturbed, incident field with the field after introduction of the object.

Figure 1 is a densigram showing the field distribution in the vicinity of man in a horizontal plane at the height of his chest. On the illuminated side a pattern of standing waves of generally parabolic shape is readily seen, and the microwave shadow region is well defined.

An attempt is made to relate these observations to a comprehensive theoretical and experimental data base concerning similar fields around inanimate objects. King and Wu (1) calculated the scattering and diffraction of electromagnetic waves by conductive and dielectric objects. Some of this information is redrawn in Figure 2 to present the field pattern for interaction of a plane wave and a conductive cylinder with axis parallel to the electric field and a cylinder diameter equal to the wavelength. The standing waves

WHO – BIOLOGIC EFFECTS & HEALTH HAZARDS OF MICROWAVE RADIATION
1974

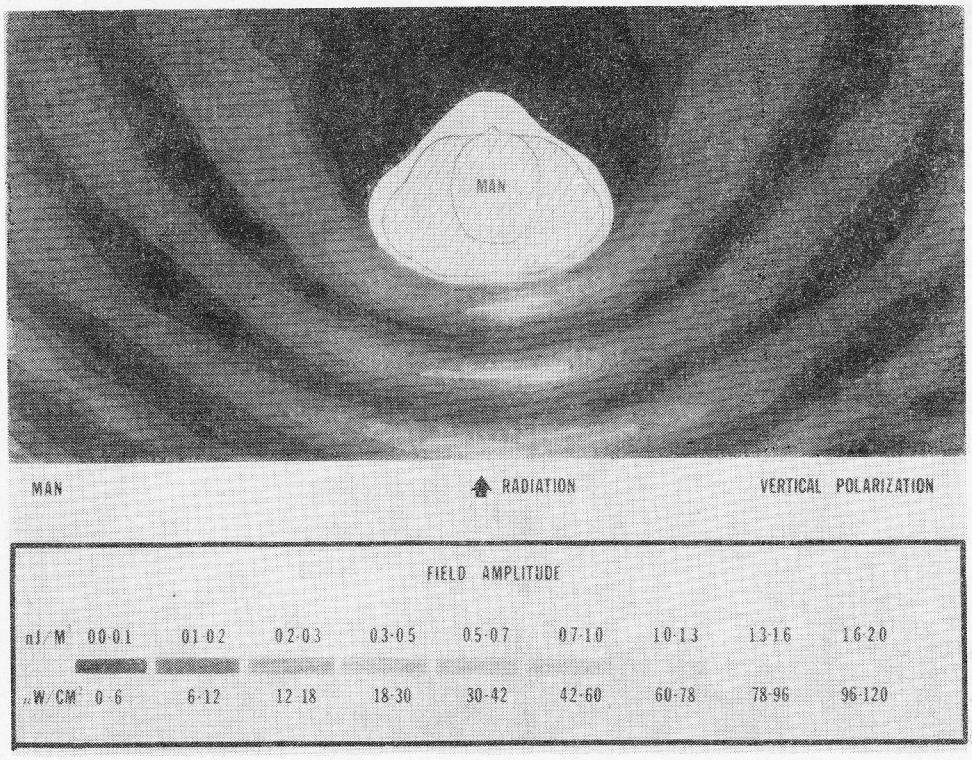

Fig. 1. Spatial energy distribution in the vicinity of man in a plane wave microwave field 1 GHz.

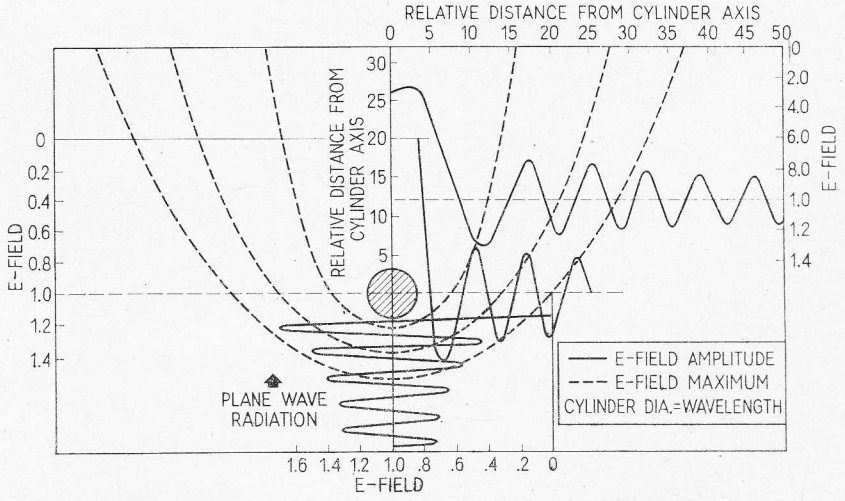

Fig. 2. Electric field near a conductive cylinder redrawn from King and Wu (1).

WHO – Biologic effects & health hazards of microwave radiation
1974

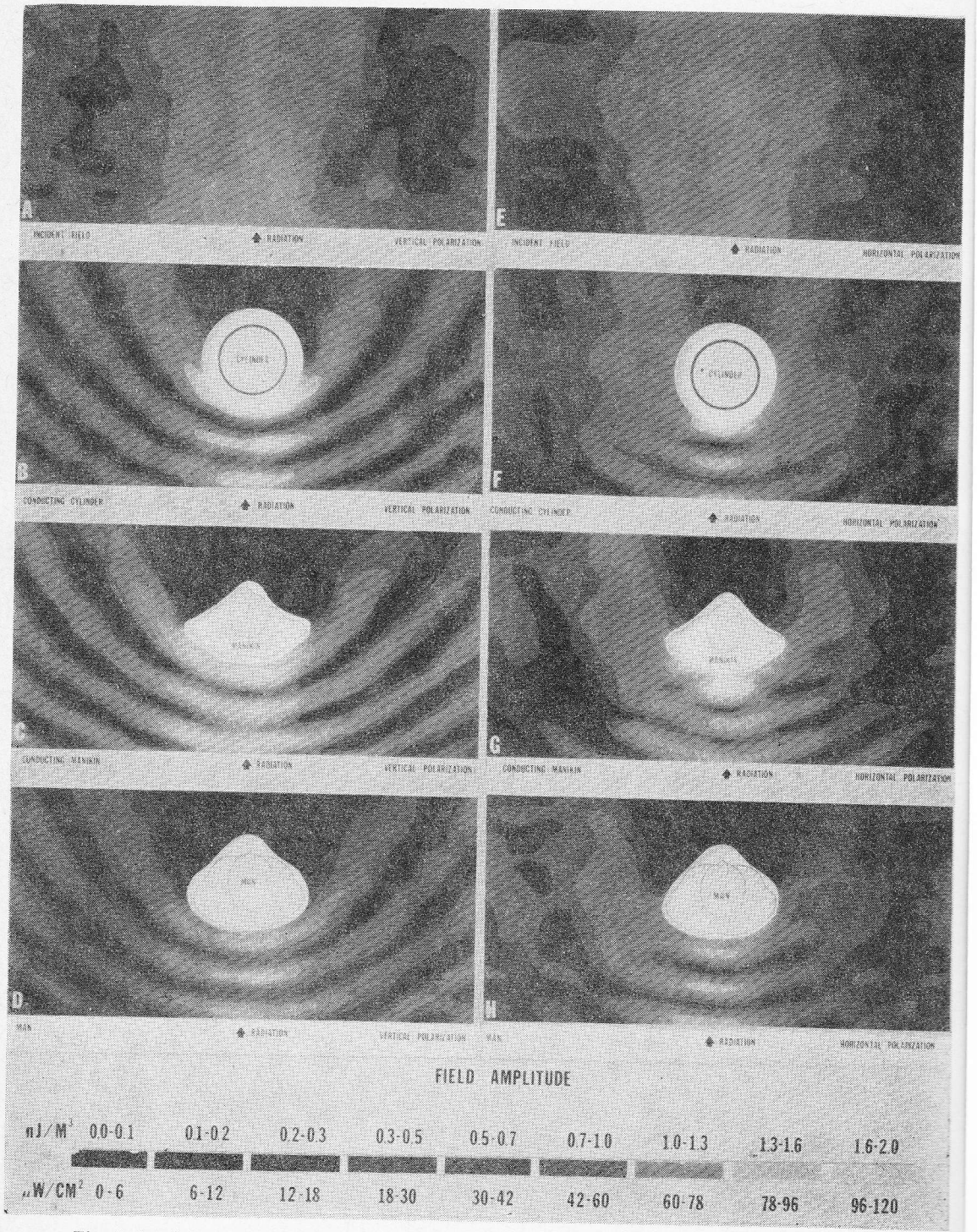

Fig. 3. Spatial energy distribution at 1 GHz (contour presentation). Row A—D Vertical polarization; Row E—H Horizontal polarization; A and E Incident field; B and F Conductive cylinder; C and G Conductive manikin; D and H man.

WHO – BIOLOGIC EFFECTS & HEALTH HAZARDS OF MICROWAVE RADIATION 1974

on the illuminated side and at two other locations are represented by dashed lines showing the parabolic curves of amplitude maxima of the electric field. These calculated curves appear similar to the pattern in Figure 1, but the shape and electrical properties of man are sufficiently different from a metal cylinder to merit special consideration. Field measurements in the vicinity of a male life-size manikin with a metallized surface were used to evaluate the influence of shape. A future comparison of the measurements on the conductive manikin with the results for a man of approximately the same shape is expected to show the influence of the electric properties of man.

Figure 3 gives a comparison of the fields measured in the vicinity of a conductive cylinder, a conductive manikin, and man for vertical and horizontal polarization and includes the incident field patterns. Figure 3 demonstrates clearly how the energy distribution is affected by the specific objects and by the polarization of the radiation. If accurate dosimetry in proximity to an object is desired, the standing wave patterns should be kept in mind. Power measurements in proximity to man for purposes of safety monitoring may be subject to gross errors in interpretation if the diffracted fields are not taken into consideration. This is true for personal dosimeters as well as for hand-held monitoring devices. Since the distance between intensity maxima in the standing wave is related to the wavelength, the positioning of the dosimeter sensor is also dependent on frequency.

The effects of polarization are easily seen in Figure 3. If the electric field is parallel to the long axis of the object (vertical polarization), the structure of the parabolic field extends a considerable distance to the side of the object, while in horizontal polarization, the side structure is low in amplitude. It can be seen that this structure is of significance if men are exposed side by side.

Curves depicting the E-field maxima calculated by King and Wu (1) for a cylinder illuminated by a plane wave and measured in our experiments with the cylinder, manikin and man are superimposed in Figure 4. The degree of correlation between the diffraction fields under the different conditions is immediately apparent. The relationship between the wavelength of the radiation and the diffraction pattern can be clearly seen on the line labeled "incident beam" where the peaks occur at intervals of one-half

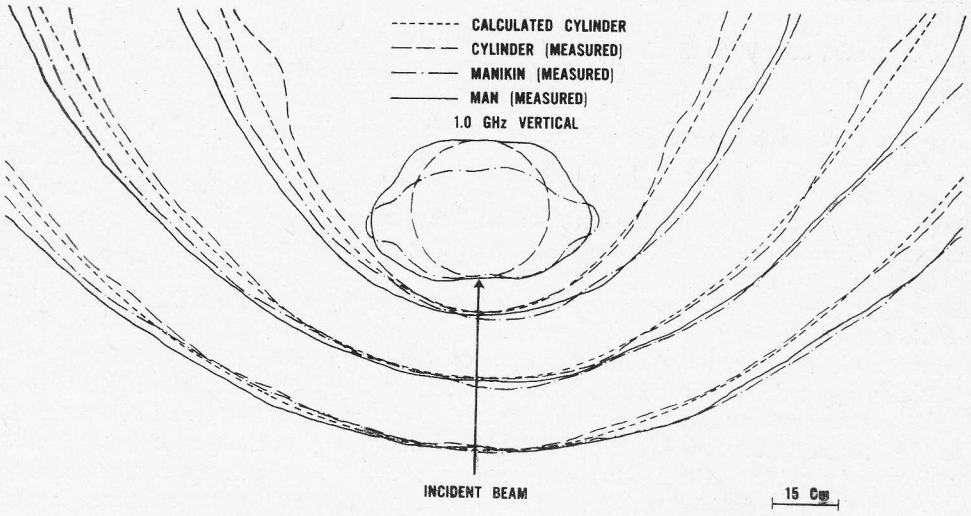

Fig. 4. Electric field maxima near diffracting objects.

WHO – BIOLOGIC EFFECTS & HEALTH HAZARDS OF MICROWAVE RADIATION 1974

wavelength. Figure 4 also shows that the effects of subject shape differences are at a minimum on the line labeled "incident beam".

A few additional observations may be of interest. The amplitude of the standing wave peaks on the beam axis diminishes with distance from the conductive cylinder and metallized manikin as is theoretically expected. If man is the scattering object, these amplitudes remain constant with distance. The difference in the two scattering patterns is best seen in A and B in Figure 5 where the information of C and D in Figure 3 is presented in a three-dimensional plot. The sagittal plane of the manikin and man is drawn in Figure 5. King and Wu (1) derived that in the case of reflection of a plane wave from an infinite, conductive plane, the amplitude of the reflected wave does not change with distance from the reflecting surface. The center of the back of man appears to act to a certain degree as an infinite conductive plane and not like a conductive cylinder. The significance of this observation has yet to be determined.

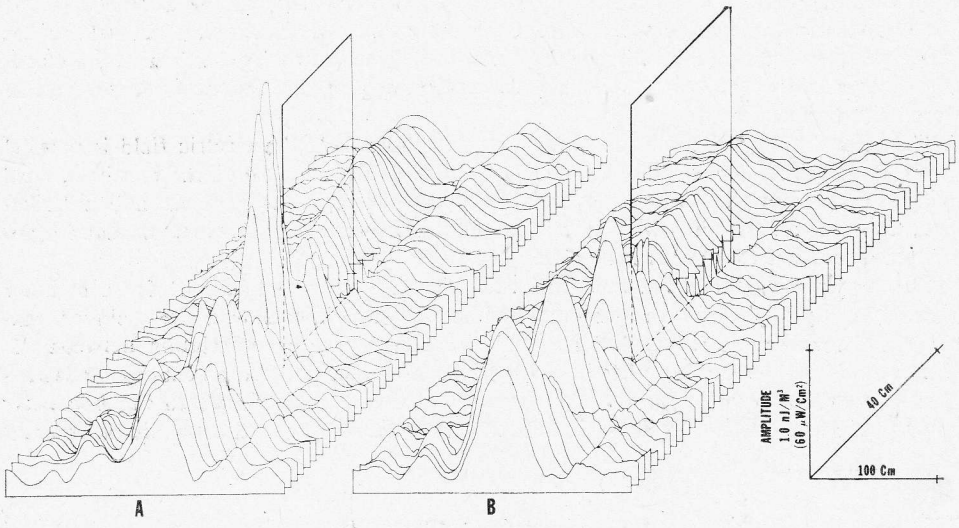

Fig. 5. Spatial energy distribution around a conducting manikin (A) and man (B). The position of the sagittal plane is indicated.

It should be pointed out in this connection that the output of the isotropic sensor at any point in space contains both phase and amplitude information about that point exactly analogous to that contained in an optical hologram. In the near future we hope to furnish additional information on the absorption of microwave energy by man by a judicious application of microwave holographic techniques.

It should be emphasized that all the studies described here, as well as others currently underway, are based upon direct measurements on human subjects. The high sensitivity of the instrumentation permits measurements to be made at the very low power levels accepted as safe for exposure of the general population. It is our belief that this approach will provide information concerning the interaction of man with a microwave environment that can be obtained by no other presently available method. In the limited space available we could indicate only the potentialities of an approach which may provide the basis for a non-invasive method to estimate the energy actually absorbed from an incident microwave field by different body parts and tissue layers of man.

REFERENCES

1. KING R. W. P., WU T. T.: *The Scattering and Diffraction of Waves.* Chap. 2. Harvard University Press, Cambridge, Mass., USA, 1959.
2. WACKER P. F., BOWMAN R. R.: *IEEE Trans. on Microwave Theory and Tech.*, 1971, MTT-19, 179.

WHO – Biologic effects & health hazards of microwave radiation
1974

WHO – Biologic effects & health hazards of microwave radiation
1974